



## Cyclopentane combustion. Part II. Ignition delay measurements and mechanism validation

Title	Cyclopentane combustion. Part II. Ignition delay measurements and mechanism validation
Author(s)	Al Rashidi, Mariam J.;Mármol, Juan C.;Banyon, Colin;Sajid, Muhammad B.;Mehl, Marco;Pitz, William J.;Mohamed, Samah;Alfazazi, Adamu;Lu, Tianfeng;Curran, Henry J.;Farooq, Aamir;Sarathy, S. Mani
Publication Date	2017-06-12
Publisher	Elsevier
Repository DOI	<a href="https://doi.org/10.1016/j.combustflame.2017.05.017">10.1016/j.combustflame.2017.05.017</a>

# Cyclopentane combustion chemistry. Part I: Mechanism development and computational kinetics

*Mariam J. Al Rashidi<sup>a,b\*</sup>, Marco Mehl<sup>c</sup>, William J. Pitz<sup>c</sup>, Samah Mohamed<sup>a</sup> and S. Mani Sarathy<sup>a</sup>*

<sup>a</sup> King Abdullah University of Science and Technology (KAUST), Clean Combustion Research Center (CCRC), Physical Science and Engineering Division (PSE), Thuwal, Saudi Arabia

<sup>b</sup> Department of Chemistry, College of Science, Sharjah University, P. O. Box 27272, Sharjah, UAE

<sup>c</sup> Lawrence Livermore National Laboratory, Livermore, California, USA

\*Corresponding author:

Dr. Mariam Al Rashidi  
Chemistry Department  
University of Sharjah  
M7, room 203B  
Sharjah, United Arab Emirates  
Tel: +971561248584 E-mail: [melrachidi@sharjah.ac.ae](mailto:melrachidi@sharjah.ac.ae)

## **Abstract**

Cycloalkanes are significant constituents of conventional fossil fuels, in which they are one of the main contributors to soot formation, but also significantly influence the ignition characteristics below  $\sim 900$  K. This paper discusses the development of a detailed high- and low-temperature oxidation mechanism for cyclopentane, which is an important archetypical cycloalkane. The differences between cyclic and non-cyclic alkane chemistry, and thus the inapplicability of acyclic alkane analogies, required the detailed theoretical investigation of the kinetics of important cyclopentane oxidation reactions as part of the mechanism development. The cyclopentyl + O<sub>2</sub> reaction was investigated at the UCCSD(T)-F12a/cc-pVTZ-F12//M06-2X/6-311++G(d,p) level of theory in a time-dependent master equation framework. Comparisons with analogous cyclohexane or non-cyclic alkane reactions are presented. Our study suggests that beyond accurate quantum chemistry the inclusion of pressure dependence and especially that of formally direct kinetics is crucial even at pressures relevant for practical application.

## **Keywords**

Cyclopentane, detailed mechanism, computational kinetics, pressure-dependent rate constants

## 1. Introduction

Cycloalkanes are important constituents of petroleum-derived liquid fuels. They make up ~40 wt% of diesel [1, 2], ~20 wt% of kerosene [3, 4], and ~10 to 15 wt% of gasoline [5]. Some studies have shown that at high temperatures, cycloalkanes may contribute to the production of soot by means of de-hydrogenation reactions [6]. Generally, cycloalkanes exhibit less low-temperature reactivity than their non-cyclic counterparts due to the conformational inhibition of the alkylperoxy $\leftrightarrow$ hydroperoxyalkyl isomerization, an important low-temperature chain branching pathway. Yang et al. [7, 8] have shown that in the case of cyclohexane, the suppression of low-temperature isomerization renders the HO<sub>2</sub>-elimination pathway more important. This leads to higher concentrations of olefins, which reduces reactivity, delays ignition and also promotes soot formation [7]. The ring strain energy changes the oxidation kinetics, particularly for the ring-opening reactions, which also involve significant change in entropy [8]. Furthermore, unlike in *n*-alkanes, methyl substitution in cycloalkanes increases low-temperature reactivity [9] for reasons that are not well known on the molecular level. Therefore, more detailed kinetic research is needed to better explain the observed trends, and to enable accurate predictive modeling of cycloalkane-containing fuels.

Due to their simplicity and abundance, particularly in shale- and oil sand-derived fuels [10], cyclohexane and cyclopentane are often used to represent the naphthenic fraction in surrogate fuels. While models for cyclohexane [11-14] cover a wide temperature range, the cyclopentane models currently available in the literature are limited to high-temperature [15, 16]. The rate coefficients of elementary reactions in these mechanisms are mostly based on analogies with cyclohexane due to the lack of cyclopentane-relevant kinetic data.

Kinetic determinations pertaining to cyclopentane reactivity are mostly concerned with high-temperature pathways such as unimolecular decomposition [17], H-abstraction by OH [18-20], and the  $\beta$ -scission of C-C and C-H bonds in cyclopentyl radicals [21-24]. Only Sirjean et al. [25] provide kinetic data of low-temperature cyclopentane reactivity. Specifically, they report high-pressure limit rate constants of cyclopentylperoxy (ROO) reactions, including alkylperoxy $\leftrightarrow$ hydroperoxyalkyl isomerization (ROO $\leftrightarrow$ QOOH) and cyclic ether formation, calculated at the CBS-QB3 level of theory. However, considering the importance of formally direct (aka well-skipping) pathways even at high pressures, as

demonstrated by Fernandes et al. [11] for cyclohexane, pressure-dependent rate coefficients are needed for accurate predictions of reactivity under a wide range of conditions. Rate constants of the hydroperoxycyclopentyl (QOOH), HO<sub>2</sub>-elimination, and  $\beta$ -scission pathways are also needed.

This study is concerned with the development of a detailed cyclopentane combustion mechanism comprising high- and low-temperature reaction pathways. The pressure-dependent kinetics of the low-temperature oxidation reactions lying on the potential energy surface (PES) of cyclopentyl + O<sub>2</sub> is determined using *ab-initio* methods and Master Equation (ME) analysis. The calculated rate constants are compared to those available in the literature for cyclopentane, as well as to those of analogous cyclohexane or non-cyclic alkane reactions. To the best of our knowledge, this work provides the first reported comprehensive chemical kinetic model for cyclopentane. The model developed herein allows for the prediction of the ignition properties of cyclopentane-containing fuels, and gives further insight into the differences between *n*-alkane and cycloalkane reactivity trends.

## 2. Mechanism development and computational methods

Our detailed mechanism of low- and high-temperature cyclopentane oxidation was developed based on the reaction scheme proposed by Sarathy et al. for 2-methyl alkanes [26]. The updated C<sub>0</sub>-C<sub>4</sub> chemistry from NUI Galway's AramcoMech 1.4 was used as base chemistry in the model [27]. The cyclohexane and methylcyclohexane sub-mechanisms from [14] and [13], respectively, were included in the model for the purpose of elucidating the effect of ring size and ring substitution on reactivity. Overall, the cyclopentane sub-mechanism consists of 148 reactions and 33 species, while the complete mechanism consists of 6816 reactions and 1598 species. The dictionary of species names and molecular structures is available in the Supplementary Material along with the mechanism and thermodynamic data files.

In our mechanism, the rate coefficients of most elementary reactions were taken from the literature, if available, or estimated based on analogies. However, in light of the above-mentioned differences between cyclic and non-cyclic alkane low-temperature kinetics [7, 8], reliable estimates of the kinetic parameters could not be made for cyclopentyl + O<sub>2</sub> with

analogies. Therefore, the kinetics of important low-temperature oxidation pathways that affect the autoignition quality of a fuel [11] and that lie on the PES of cyclopentyl + O<sub>2</sub> were determined computationally in this current paper. The rate coefficients of cyclopentyl scission reactions were also determined computationally, because although several studies available in the literature are concerned with the estimation or computation of these reaction rates, the reported values are not in good agreement with each other [15, 21, 23, 24]. Considering that the C-C/C-H scission branching ratio and kinetics have a great influence on the fuel concentration profile [28], and thus, on reactivity, it was necessary to recalculate the rate coefficients of these reactions at a higher level of theory than the earlier studies. Further details regarding the computed parameters for scissions and how they compare to the literature values may be found in Ref. [28].

Simplified schemes of the high- and low-temperature cyclopentane oxidation mechanisms are depicted in Figures 1 and 2, respectively. A detailed account of the kinetics used for the reaction classes appearing in these schemes is given below.

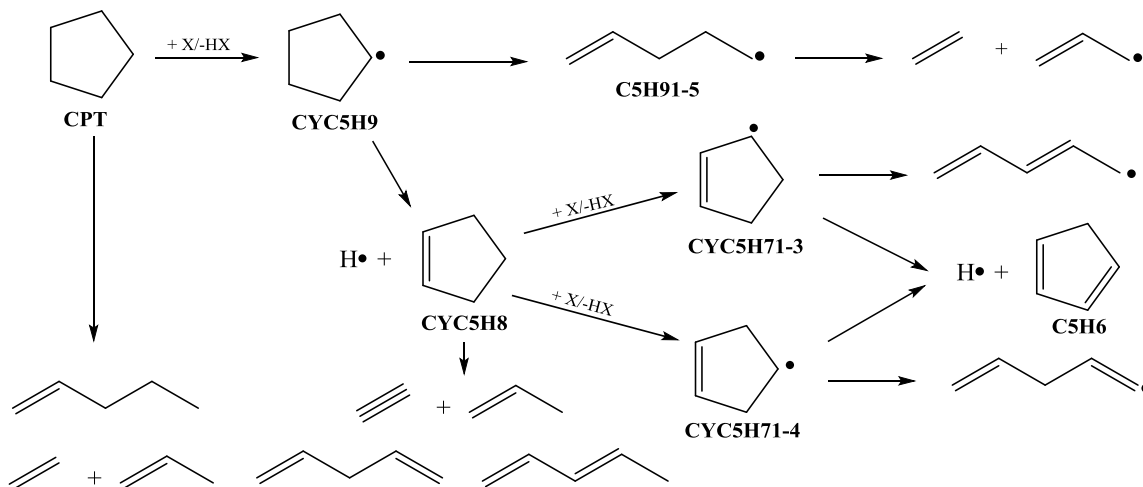


**Figure 1.** Schematic high-temperature cyclopentane decomposition pathways. X is H, O, OH, O<sub>2</sub>, HO<sub>2</sub>, CH<sub>3</sub>, CH<sub>3</sub>O<sub>2</sub>, CH<sub>3</sub>O or C<sub>2</sub>H<sub>5</sub>.

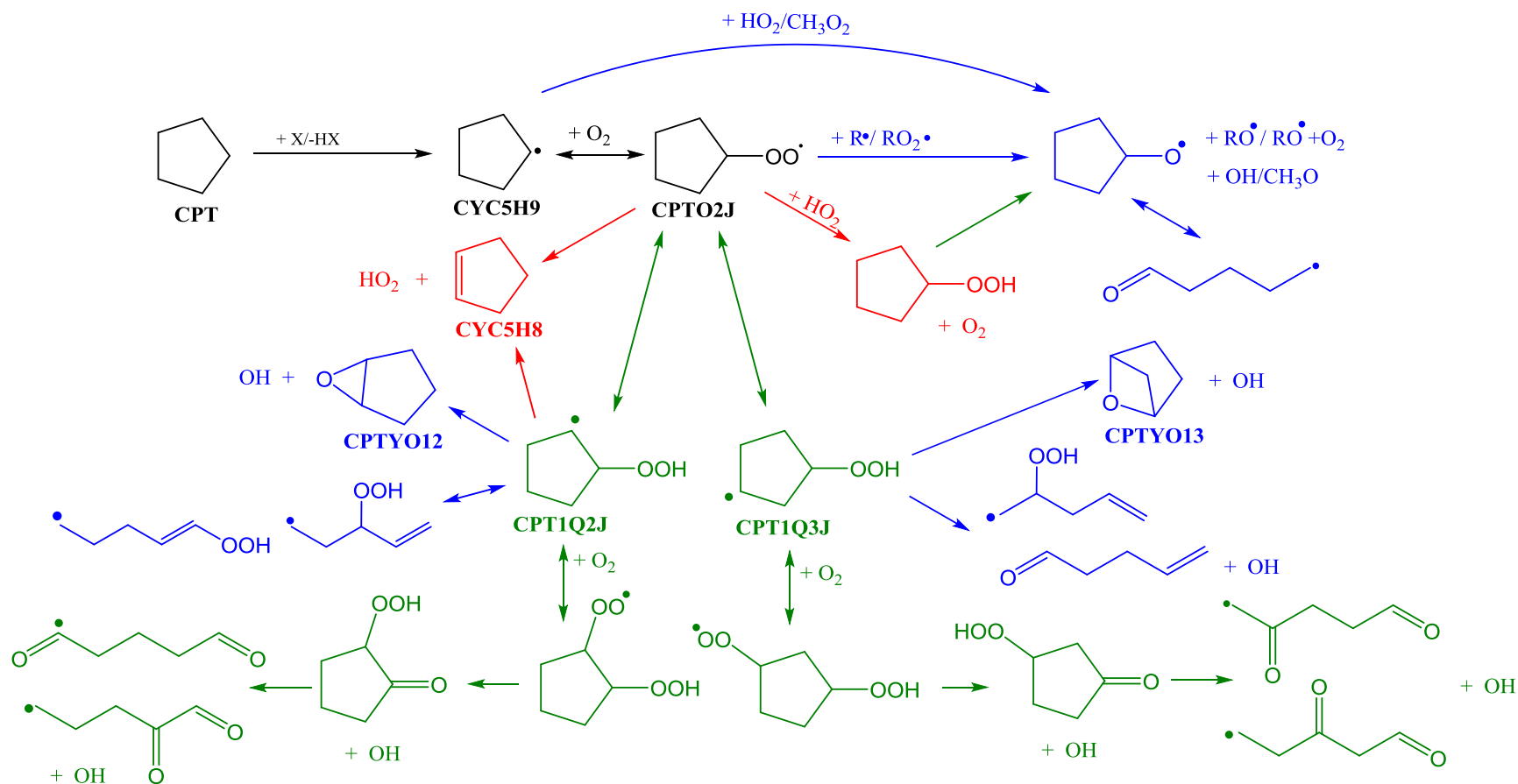


**Figure 2.** Schematic low-temperature oxidation mechanism of cyclopentane. Pathways colored in red, blue and green represent chain termination, propagation and branching pathways, respectively. X is H, O, OH, O<sub>2</sub>, HO<sub>2</sub>, CH<sub>3</sub>, CH<sub>3</sub>O<sub>2</sub>, CH<sub>3</sub>O or C<sub>2</sub>H<sub>5</sub>.

### 2.1. Unimolecular decomposition

In our detailed mechanism, the unimolecular decomposition pathways of cyclopentane include fission reactions to form 1-pentene, ethene + propene, and cyclopentyl radical + H. Similar to the high-temperature cyclopentane mechanisms of Tian et al. [16] and Sirjean et al. [15], the rate coefficients of these reactions are taken from the shocktube experiments of Tsang [17]. The same rate coefficients were used for the unimolecular decomposition reaction of cyclopentene to 1,4-pentadiene as for cyclopentane, except, the activation energies were corrected to account for the difference in bond dissociation energies (BDE) between vinylic-secondary (cyclopentene) and secondary-secondary (cyclopentane) bonds, as well as for the difference between cyclopentene and cyclopentane ring strain: 0.8 kcal mol<sup>-1</sup>, calculated at the CBS-QB3 level of theory [29]. These ring strain values were extracted by Ritter [30] from thermodynamic evaluations of cyclic species by Dorofeeva et al. [31]. The BDE correction was estimated as 12.8 kcal mol<sup>-1</sup> by analogy with  $\Delta$ BDE of  $n\text{-C}_4\text{H}_{10} \rightarrow \text{C}_2\text{H}_5 + \text{C}_2\text{H}_5$  and  $1\text{-C}_4\text{H}_8 \rightarrow \text{C}_2\text{H}_3 + \text{C}_2\text{H}_5$ . The pathway cyclopentene  $\rightarrow$  1,3-pentadiene, where 1,3-pentadiene is a lumped species (1,3-pentadiene and vinylcyclopropane) has also been included. This reaction involves the generation of a resonantly stabilized allylic di-radical, and its activation energy was estimated by analogy with 1-pentene = ethyl + allyl. A correction factor of -5.1 kcal corresponding to the destabilizing ring strain energy in cyclopentene was applied. The thermal decomposition of the C-H bond in cyclopentane was written in the exothermic recombination direction, and the recommended rate constants of Allara and Shaw [32] were used. Finally, rate coefficients from Lewis et al. [33] were used for H<sub>2</sub> elimination from cyclopentene (included in the mechanism, but not shown in Figure 1).

### 2.2. H-abstraction

The H-abstracting species that were taken into consideration are H, O, OH, O<sub>2</sub>, HO<sub>2</sub>, CH<sub>3</sub>, CH<sub>3</sub>O<sub>2</sub>, CH<sub>3</sub>O and C<sub>2</sub>H<sub>5</sub> (referred to as X in Figures 1 and 2). The rate coefficients of the abstraction reactions were assigned based on Sarathy et al.'s [26] rate rules for H-abstraction from secondary sites, except in the case of H-abstraction by OH. Although several experimental and theoretical studies of H-abstraction by OH from cyclopentane exist in the literature [18, 20, 34-40], most of them are limited to a narrow temperature

range ( $< 500$  K) [18, 36, 37, 39, 40] or even just to a single temperature [34, 35, 38]. In this work we used rate coefficients for the cyclopentane + OH reaction based on the work of Sivaramakrishnan and Michael, who investigated this reaction using shocktube experiments between 813 to 1341 K [20]. The measured rate constants were combined with lower-temperature experimental data available in the literature, and then fitted to a modified Arrhenius equation. They also used high level electronic structure calculations to extrapolate the rate constants over an even wider range of temperatures (250-2000 K). The two expressions resulting from experimental data and computations yield rate constants that differ by only up to 15% in the 813 – 1341 K temperature range for which rate constants are directly measured in the shocktube [20]. Below 813 K they are within 7% of each other. The calculated rate constant values from Ref. [20] are also in good agreement with those obtained using our rate rule [26] ( $< 50\%$  different between 250 and 2000 K), as well as with those reported by Handford-Styring and Walker [19] ( $< 10\%$  different between 250 and 2000 K). The experimentally-derived rate coefficient values from Ref. [20] were used in the mechanism.

Unlike cyclopentane, cyclopentene has three different abstraction sites: vinylic, allylic and secondary. The abstraction rate coefficients from the secondary and allylic sites were equated on a per-H-atom-basis by those from cyclopentane and 1-hexene [41], respectively, while abstraction from the vinylic sites was neglected because of the high barrier.

### 2.3. $\beta$ -scission

References [21], [22], [23] and [24] provide rate coefficients for C-H and C-C (ring opening)  $\beta$ -scission reactions of the cyclopentyl radical (CYC5H9). These rate coefficients were determined at the CBS-QB3 level of theory [22, 24] using a QRRK/MSM model to evaluate the pressure dependence [24], using shocktube measurements of the C-C/C-H branching ratio [21], or using simpler estimates [23]. The rate coefficients in these studies differ by up to a factor of 16, which is concerning, especially considering that high-temperature ignition and species concentration profiles [28, 42] are highly sensitive to the rates of these scission reactions. Moreover, none of the reported values could reproduce our experimental speciation profiles adequately [28]. Therefore, we recalculated the high-

pressure limit rate constants of cyclopentyl C-H and C-C scission at the CCSD(T)-F12a/cc-pVTZ//M06-2X/6-311++G(d,p) level of theory. Hindered rotor corrections were included for the C5H9-5 product at the M062X/6-311++G(d,p) level of theory using 20° increment scans. However, tunneling corrections were not included. The pressure-dependence of these reactions was estimated based on the falloff parameters of Ref. [24]. Further details regarding the calculated rate constants and how they compare to the literature values may be found in [28].

The ring-opening reactions of cyclopentyl radicals were written in the exothermic reverse direction, and Matheu et al.'s [43] rate constants of 1,5 endo intramolecular addition were used. Activation energy corrections of -13 and +8 kcal mol<sup>-1</sup>, corresponding to differences in bond dissociation energies, were applied to account for vinyl radical destabilization and allyl radical stabilization compared to secondary radicals, respectively. Considering that Matheu et al.'s [43] recommendations were proposed for a system with more rotational degrees of freedom than ours, the pre-exponential factors of C5H7-1  $\rightleftharpoons$  CYC5H7-4 and C\*CC\*CCJ  $\rightleftharpoons$  CYC5H7-3 were multiplied by factors of 8 and 8<sup>3</sup>, respectively, where the factor of 8 corresponds to the approximate entropy loss from one CH<sub>2</sub> rotor being “tied up” in the cyclic transition state. This factor is based on the approximate reduction in A-factor from the loss of one rotor in going from a 4-membered to a 5-membered RO<sub>2</sub> isomerization transition state [44]. The C-H scission reactions were also written in the exothermic reverse direction, and the rate coefficients were assigned to be the same as H-addition to propene [45].

#### *2.4. O<sub>2</sub>-addition to cyclopentyl, alkylperoxy $\leftrightarrow$ hydroperoxyalkyl isomerization, HO<sub>2</sub>-elimination, cyclic ether formation, and $\beta$ -scission of hydroperoxyalkyl radicals*

Previous studies have shown that cycloalkane low-temperature reactivity is different from that of *n*-alkanes due to the ring strain energy and frozen rotors imposed by the cyclic structure [7, 8, 46, 47]. Therefore, the use of non-cyclic hydrocarbon analogies in the estimation of naphthenic reactivity is inappropriate. Moreover, since reactivity strongly depends on the ring size, analogies with other cyclic species, such as the widely investigated cyclohexane [14, 48, 49], are also inaccurate.

O<sub>2</sub>-addition to cyclopentyl, alkylperoxy $\leftrightarrow$ hydroperoxyalkyl isomerization, HO<sub>2</sub>-elimination, cyclic ether formation, and  $\beta$ -scission of hydroperoxyalkyl radicals collectively happen on the PES of cyclopentyl+O<sub>2</sub>. In this study, we calculated the rate constants for these reactions at the UCCSD(T)-F12a/cc-pVTZ-F12//M06-2X/6-311++G(d,p) level of theory and used them in our mechanism. Details of these calculations are given here in Section 3. Importantly, formally direct pathways on the PES of cyclopentyl + O<sub>2</sub> that have a significant effect on cyclopentane reactivity have also been incorporated into the mechanism, including CYC5H9+O<sub>2</sub>=CPT1Q2J and CYC5H9+O<sub>2</sub>=CPT1Q3J. The reaction of CYC5H9+O<sub>2</sub>=CYC5H8+HO<sub>2</sub> is included as a formally direct as well as a direct abstraction pathway, although the direct abstraction reactions were not found to have a significant effect on reactivity.

For the addition of O<sub>2</sub> to QOOH (“second O<sub>2</sub> addition”) we used the same rate coefficients as for the O<sub>2</sub>-addition to the cyclopentyl radical. However, the pre-exponential factors of the second addition were divided by 2 based on analogy with propyl + O<sub>2</sub> reaction [50]. Also, the rate coefficients of the OOQOOH isomerization reactions were assigned by analogy with the alkylperoxy $\leftrightarrow$ hydroperoxyalkyl isomerization reactions, but only the isomerization reactions leading to the formation of ketohydroperoxides were considered. Activation energy corrections of -8.6 and -2.2 kcal mol<sup>-1</sup> were applied to 1,4 and 1,5 migration reactions in order to account for the effect of the -OOH group on the C-H bond strength at the  $\alpha$ -site. These correction values are taken from the computational work of Sharma et al. [51]. Alternative isomerization pathways were found not to have an effect on low-temperature ignition; and thus, these pathways were neglected.

### 2.5. Decomposition of alkylhydroperoxides and ketohydroperoxides

Ketohydroperoxides are important intermediates in low-temperature chain branching reactions. They decompose via O-O bond scission to produce alkoxy and OH radicals. Sarathy et al. [26] used an activation energy of this type of reaction of 39 kcal mol<sup>-1</sup> to simulate the low temperature ignition of acyclic alkanes. More recently, Jalan et al. [52] calculated the rate constants of a C3-ketohydroperoxide decomposition at the RCCSD(T)-F12a/cc-pVTZ-F12//M06-2X/MG3S level of theory. They determined that the activation energy is 43 kcal mol<sup>-1</sup> for the homolytic O-OH scission of the studied KHP (the

asymptotic energy for this barrierless reactions is 49.5 kcal mol<sup>-1</sup>). In subsequent studies of low-temperature hydrocarbon oxidation, the activation energy of 43 kcal mol<sup>-1</sup> was found to be too high, and was reduced to 41.6 kcal mol<sup>-1</sup> in order to better match the experimental ignition delay data of *n*-hexane and pentane fuels [53, 54]. In this study, we evaluated the effect of using these various values (39, 43 and 41.6 kcal mol<sup>-1</sup>) on cyclopentane reactivity at a pressure of 20 bar and equivalence ratio of 1. For temperatures higher than 750 K, the exact value of the activation energy did not influence the overall reactivity. However, between 650 and 750 K, the use of 43 and 41.6 kcal mol<sup>-1</sup> activation energy slowed the reactivity by 30 and 15 % relative to that obtained when using a value of 39 kcal mol<sup>-1</sup>. All three values gave reasonable agreement with the experimental shocktube and rapid compression machine (RCM) results presented in part II of this study. Jalan et al.'s [52] rate coefficients of ketohydroperoxide decomposition were used in the final version of the model. The same activation energies were used for the decomposition of alkylhydroperoxide species as well. The Korcek decomposition [52] of the ketohydroperoxide via a cyclic peroxide intermediate was found to reduce reactivity by only 11% at 700 K, and thus, was neglected.

### 2.6. Miscellaneous reactions

Other reaction classes were also included in the mechanism such as the addition of O and OH radicals to unsaturated bonds (cyclopentene), the reactions of alkyl and alkenyl radicals with HO<sub>2</sub>, CH<sub>3</sub>O<sub>2</sub> and C<sub>2</sub>H<sub>5</sub>O<sub>2</sub>, the decomposition of cyclopentoxy radical, and H-abstraction followed by unimolecular reactions of cyclic ethers and cyclic aldehydes.

## 3. Computational methods

The reaction pathways of the cyclopentyl radical + O<sub>2</sub> adduct (ROO, shown in Figure 3) were traced to hydroperoxy alkyl radicals (QOOH), cyclic ethers,  $\beta$ -scission products, and HO<sub>2</sub> elimination products. The geometries and harmonic frequencies of the minima and saddle points were calculated at the M06-2X/6-311++G(d,p) level of theory. Minimum energy conformers were determined with the aid of 1-D relaxed scans performed at the B3LYP/6-31+G(d,p) level of theory along all relevant dihedrals. The cyclopentyl backbone had always just one stable conformer, unlike the cyclohexyl backbone [12], which

simplified the conformational search. Single point electronic energies were calculated at the UCCSD(T)-F12a/cc-pVTZ-F12 level of theory [55] and we characterized the hindered rotors of the minimum energy conformers using relaxed scans with dihedral angle increments of  $20^\circ$  at the M06-2X/6-311++G(d,p) level of theory. The expected uncertainty in the UCCSD(T)-F12 energies is 1-2 kcal mol<sup>-1</sup> for structures with moderate multi-reference character. Dihedral scans, geometry, and frequency calculations were done with the Gaussian 09 suite of programs [56], whereas the MOLPRO software [55] was used for the single point CCSD(T)-F12 calculations.

The number of states for the barrier-less O<sub>2</sub> addition step was treated using variable-reaction-coordinate transition state theory (VRC-TST) [57-59]. The inter-fragmental potential of the rigid fragments were sampled at the CASPT2(7e,5o)/cc-pVDZ level [55]. The active space consists of electrons in the  $\pi$  orbitals of O<sub>2</sub>, as well as the radical electron in cyclopentyl. We applied a distance-dependent (1-D) correction to the sampled energies that included geometry relaxation, zero-point, and basis-set effects. The basis set correction meant an extrapolation to the complete basis set from the aug-cc-pVDZ and aug-cc-pVTZ basis sets. At close distances (3-6.5 bohr interpivotal separation) two pivot points were placed on the O<sub>2</sub> molecule along the O–O axis displaced by 0.5 bohr outside the O atoms, and two pivot points on the cyclopentyl radical 1 bohr above and below the radical center. Between 7 and 15 bohr interpivotal distances the pivot points were simply placed on the center of mass of the fragments. We sampled about 9000 points in total.

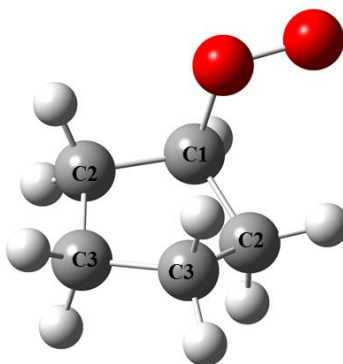


**Figure 3.** Optimized geometry of the minimum energy conformer of the cyclopentylperoxy radical.

The pressure- and temperature-dependent rate coefficients of all investigated reactions, including those of the formally direct ones, were determined by solving the time-dependent multiwell master equation for the temperature range 300-1200 K, at pressures of 0.001, 0.01, 0.1, 1, 10 and 100 bar. In these calculations tunneling corrections were included using Eckart barriers, and the state counts also included the 1-D separable hindered rotor representation of the conformational space. All frequencies not associated with hindered rotors were treated as harmonic and unscaled. We used the empirical  $\langle \Delta E_{\text{down}} \rangle = 200 \times (T/300)^{0.85} \text{ cm}^{-1}$  exponential-down energy transfer parameterization. Almost all species on the cyclopentyl + O<sub>2</sub> PES have an external rotational symmetry number  $\sigma$  of 0.5 due to non-identical mirror images, except for CYC5H9 ( $\sigma = 2$ ), O<sub>2</sub> ( $\sigma = 2$ ), CPTO2J ( $\sigma = 1$ ), CPTO2J $\leftrightarrow$ CPT1O ( $\sigma = 1$ ), CPT1O ( $\sigma = 2$ ), CYC5H8 ( $\sigma = 2$ ), CPTYO12 ( $\sigma = 1$ ), CPTYO13 ( $\sigma = 1$ ), and PT1N1Q5J ( $\sigma = 1$ ). It should be noted that in a strict harmonic picture the symmetry number of cyclopentyl is 1 and not 2. However, due to the low puckering barrier of this species, and in order to avoid an over-count of states, a symmetry number of 2 is used. Ideally, anharmonic motions of the cyclopentyl radical should be included in the state count. The ME was solved using the MESS (Master Equation System Solver) code [59]. The rate coefficients were calculated using the eigenvector-eigenvalue method of Miller and Klippenstein as described in Ref. [59], including rigorous well-merging that is necessary at higher temperatures. The phenomenological rate coefficients were fit to single and double Arrhenius parameters at various pressures using the MESS\_TPfit code of Goldsmith [59] in the 300 – 1200 K range. The Lennard-Jones parameters for all wells were set to  $\epsilon = 523.2 \text{ cm}^{-1}$  and  $\sigma = 5.7 \text{ \AA}$ , estimated based on the critical temperatures and pressures of CPTO2H according to the correlations developed by [60].

#### 4. Thermodynamic data

The thermodynamic properties of new species were calculated using Benson's group additivity methods [61] implemented in the THERM software [30], except for those involved in the PES of cyclopentyl + O<sub>2</sub> whose properties were determined using the calculated energies, frequencies and rotational barriers. Table 1 lists the computed thermochemical properties of these species, as well as formation enthalpies calculated

using THERM. As shown in Table 1, the differences between the two sets of enthalpy values are up to 2 kcal mol<sup>-1</sup>, which is within the estimated uncertainty limit of the computational enthalpy values ( $\pm 1$ -2 kcal mol<sup>-1</sup> as per Goldsmith et al. [62]) except for CPTYO13 where the difference is almost 6 kcal mol<sup>-1</sup>. CPTYO13 is a cyclic ether where the oxygen bridges the C1 and C3 carbon atoms of cyclopentane. Three cycles may be identified for this species (C5, C3O and C4O cycles); however, the shapes of these cycles are distorted relative to ordinary, non-bridged structures. Therefore, group additivity is not accurate for calculating the thermodynamic properties of this cyclic species. Similarly, the entropy values determined using computational methods are similar to those calculated using THERM, with differences ranging between 0.0 and 2.6 kcal mol<sup>-1</sup> K<sup>-1</sup>. The computed enthalpies are also compared to those reported by Sirjean et al. [25] obtained at the CBS-QB3 level of theory for the alkylperoxy, hydroperoxyalkyl, and cyclic ether species (Table 1). The formation enthalpies calculated in this study are consistently higher than those reported by Ref. [25], whereas deviations from THERM-calculated values are unsystematic. Such deviations greatly influence reactivity as demonstrated in Ref. [63]. The greatest differences are observed for CPTO2J species: 4.1 kcal and 3.2 kcal between the CBS-QB3 enthalpy values reported by [25] and those calculated in this study using CCSD(T)-F12a level of theory and THERM, respectively. However, the CBS-QB3 enthalpy value reported by Auzmendi-Murua and Bozelli [64] for the same species at 298 K is -9.0 kcal, which is 2.7 kcal lower than the CBS-QB3 value reported by [25], but 1.4 and 0.5 kcal higher than our values.

**Table 1.** Thermochemical values of intermediates lying on the PES of cyclopentyl+O<sub>2</sub>, calculated at the CCSD(T)-F12a/cc-pVTZ-F12//M06-2X/6-311++G(d,p) level of theory (in units of cal, mol and K) compared to values from THERM [30] and Ref. [25].

	$\Delta H_{298}$	$S_{298}$	Cp							THERM		[25]
			300	400	500	600	800	1000	1500	$\Delta H_{298}$	$S_{298}$	$\Delta H_{298}$
CYC5H9	26600	72.0	22.1	29.8	36.6	42.3	51.0	57.2	66.7	26900	72.1	-
CYC5H8	9600	69.4	19.7	27.1	33.6	39.0	47.1	52.9	61.7	7500	69.4	-
CPTO2J	-7600	82.7	27.4	36.4	44.3	50.8	60.6	67.5	77.8	-8500	82.9	-11700
CPT1Q2J	5600	85.1	30.2	38.9	46.4	52.5	61.7	68.2	77.9	4700	87.5	4300
CPT1Q3J	4100	84.7	30.3	39.0	46.5	52.6	61.8	68.2	78.0	4100	87.3	3700
CPTYO12	-20900	71.7	21.8	30.1	37.3	43.2	52.0	58.2	67.3	-20000	69.5	-22900
CPTYO13	-10900	69.9	21.0	29.7	37.2	43.2	52.1	58.2	67.3	-16900	70.0	-13400

CPT1O	-45600	75.2	23.4	31.1	38.0	43.6	52.1	58.2	67.3	-45300	77.2	-47500
C4H7CHO1-4	-24000	82.1	26.2	33.2	39.4	44.6	52.7	58.6	67.5	-24800	82.2	-
PT1N4Q5J	23300	92.8	34.1	42.0	48.8	54.3	62.7	68.7	78.1	21300	93.0	-
PT1N3Q5J	22500	92.7	34.3	42.1	48.8	54.3	62.7	68.7	78.1	24800	92.9	-
PT1N1Q5J	23500	94.0	34.0	41.8	48.5	54.1	62.5	68.6	78.1	23900	94.2	-

## 5. Results

### 5.1. Potential energy surface

The calculated stationary points on the cyclopentyl + O<sub>2</sub> potential energy surface are depicted in Figure 4. The oxidation kinetics on this surface is characterized by 132 irreversible reactions, 24 of which connect adjacent reactants, wells or bimolecular products; the rest are formally direct. Zero-point corrected energies calculated at the UCCSD(T)-F12a level of theory are reported relative to that of cyclopentyl + O<sub>2</sub>. The addition of O<sub>2</sub> leads to a chemically activated adduct that may i) form a stable alkylperoxy radical, ii) abstract internally an H-atom, or iii) undergo HO<sub>2</sub>-elimination leading to an olefin. Following the H-transfer step it is also possible to iv) form cyclic ethers + OH, or v) undergo  $\beta$ -scission reactions. As shown in Figure 4, the overall lowest energy pathways are H-migration to CPT1Q3J, formation of the 3-membered ring cyclic ether (CPTYO12) + OH, and concerted HO<sub>2</sub>-elimination. The barriers involved in these pathways are all lower than the entrance channel by at least 5 kcal mol<sup>-1</sup>. H-migration from the  $\alpha$ -carbon of ROO requires a 4-membered ring transition state that is energetically unfavorable. The  $\beta$ -scission pathways of QOOH radicals are also unfavorable with barriers at least 10 kcal mol<sup>-1</sup> above the entrance channel. Isomerizations of hydroperoxyalkyl radicals were also taken into consideration. However, both, the 3- and 4-membered ring transition states involved in the inter-conversion between the QOOH species have energies that are much higher than the entrance channel (20 and 27 kcal mol<sup>-1</sup>, respectively). Reactions with barriers higher than 15 kcal mol<sup>-1</sup> above the entrance channel were excluded from the ME analysis. Finally, the barrier height for formation of 1,3-epoxycyclopentane (CPTYO13) is relatively high compared to that of 1,2-epoxycyclopentane (CPTYO12), which is comparable to the differences in barrier heights of analogous reactions for non-cyclic alkanes [65]. This is consistent with the results reported by Sirjean et al. [25] who calculated the barriers of alkylperoxy $\leftrightarrow$ hydroperoxyalkyl isomerization and cyclic ether

formation of cyclopentane at the CBS-QB3 level of theory. They suggested that the high barrier for the formation of CPTYO13 is a result of the significant bond angle deformations required to reach the transition state, which increases the molecular strain [25]. Table 2 shows that the barrier heights calculated in this study are similar to those reported by [25], with differences smaller than  $2.4 \text{ kcal mol}^{-1}$ .



**Table 2.** Comparison of barrier heights from UCCSD(T)-F12a (this study) and CBS-QB3 (Sirjean et al. [25]) calculations at 298 K (in units of kcal mol<sup>-1</sup>)

<i>Reaction</i>	$\Delta H^\ddagger_{298}$	
	<i>UCCSD(T)</i>	<i>CBS-QB3</i>
CPTO2J=CPT1O+OH	41.7	40.6
CPTO2J=CPT1Q2J	32.3	31.1
CPTO2J=CPT1Q3J	26.8	24.4
CPT1Q2J=CPTYO12+OH	9.2	10.0
CPT1Q3J=CPTYO13+OH	23.4	23.0

### 5.2. Rate constants

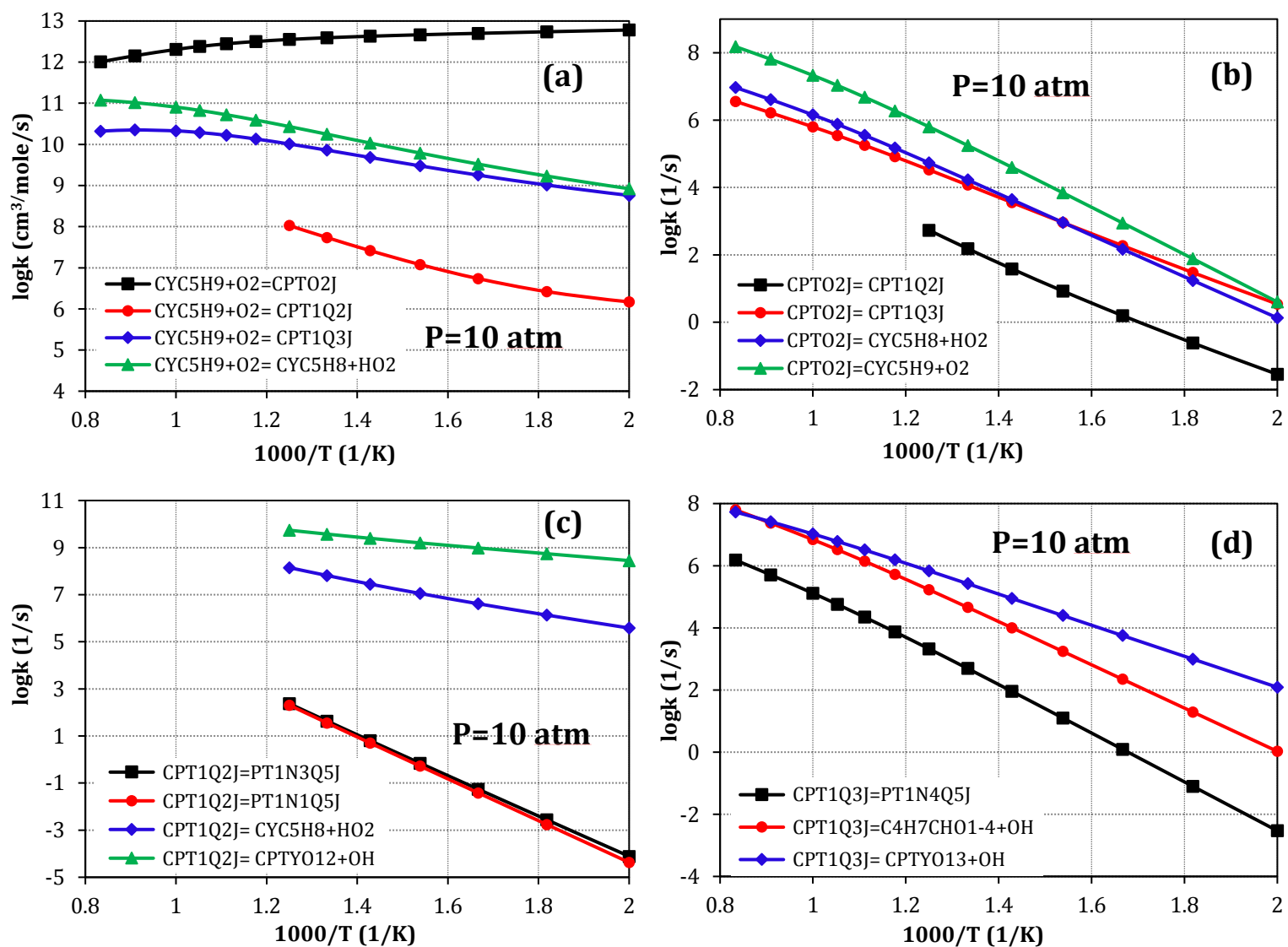
The temperature- and pressure- dependent rate constants of the investigated reactions are fitted to single as well as double modified Arrhenius equations in order to determine  $A$ ,  $n$  and  $E_a$  (pre-exponential factor, temperature coefficient and activation energy, respectively) at each pressure. The mean absolute fitting errors obtained for sequential reactions with the double Arrhenius fit are less than 16% over a fit range of  $300 \text{ K} < T < 1200 \text{ K}$ . The high-pressure limit coefficients of the single Arrhenius fits are summarized in Table 3. The rate coefficients at pressures of 0.001, 0.01, 0.1, 1, 10 and 100 bar are given in supplementary material; we provide both the fits and the raw data. In the reactor simulations we used the more accurate double Arrhenius fits (i.e., the total rate constant is the sum of two modified Arrhenius expressions), while the single Arrhenius fits are given for use in versions of CHEMKIN (or other integrators) that do not support the double Arrhenius format combined with the PLOG command. The uncertainties in the calculated rate constants are estimated to be similar to the ones established by Goldsmith et al. [62] for the propyl + O<sub>2</sub> system.

**Table 3.** High-pressure limit rate coefficients of reactions lying on the potential energy surface of cyclopentyl + O<sub>2</sub> in units of cm<sup>3</sup>, mol, s and cal,  $k = A \times (T/\text{K})^n \times e^{-E/(RT)}$ ,  $R = 1.987 \text{ cal mol}^{-1} \text{ K}^{-1}$ . The fitting range is  $300 \text{ K} < T < 1200 \text{ K}$ .

	<i>A</i>	<i>n</i>	<i>E<sub>a</sub></i>
CYC5H9+O2=CPTO2J	$9.29 \times 10^{12}$	-0.20	-800
CPTO2J=CPT1Q2J	81.2	2.98	25639
CPTO2J=CPT1Q3J	225.2	2.75	21003
CPTO2J=CYC5H8+HO2	382.3	2.95	23176
CPTO2J=CPT1O+OH	45.6	3.27	35429
CPT1Q2J=CYC5H8+HO2	1852.8	2.99	10470
CPT1Q2J=CPTYO12+OH	2120.8	2.78	4320
CPT1Q2J=PT1N3Q5J	311.2	3.18	28230

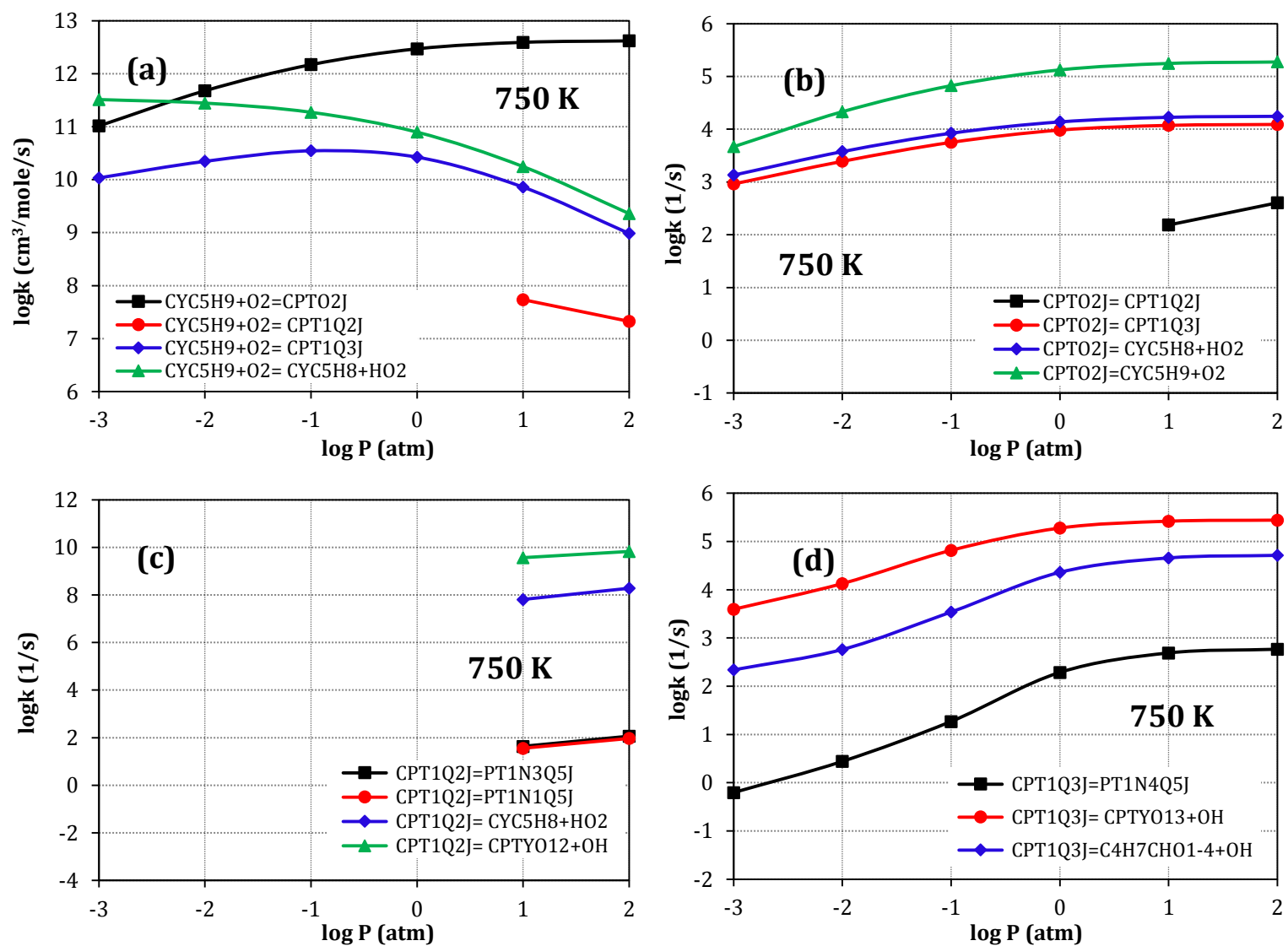
CPT1Q2J=PT1N1Q5J	325.4	3.19	28500
CPT1Q3J=CPTYO13+OH	657.5	2.74	17779
CPT1Q3J=C4H7CHO1-4+OH	865.5	3.27	25766
CPT1Q3J=PT1N4Q5J	234.8	3.20	29785

Figure 5 depicts the temperature-dependence of the calculated rate constants at a pressure of 10 bar. Figures 5a, 5b, 5c and 5d show the rate constants of reactions involving CYC5H9+O2, CPTO2J, CPT1Q2J and CPT1Q3J species, respectively. The results are presented at 10 bar because pressures of 10 to 100 bar are most relevant to practical combustion systems. The well-skipping reactions that are not shown in Figure 5 are relatively slow, and thus, unimportant. Only pathways with rate constants greater than  $100 \text{ cm}^3\text{mol}^{-1}\text{s}^{-1}$  or  $\text{s}^{-1}$  at 750 K for any of the investigated pressures were included in the mechanism. The most dominant reaction at 10 bar, up to a temperature of 1200 K, is the addition of O<sub>2</sub> to cyclopentyl to form the stabilized cyclopentylperoxy radical. The well-skipping channels of CYC5H9+O<sub>2</sub> going directly to CYC5H8+HO<sub>2</sub> or CPT1Q3J are also important over the entire temperature range with rate constants similar in magnitude to those of formation of 3-membered ring cyclic ether (CPTYO12) from CPT1Q2J. These formally direct reactions exhibit little temperature-dependence. Meanwhile, the elimination of HO<sub>2</sub> from CPT1Q2J and the well-skipping pathway of CYC5H9+O<sub>2</sub>=CPT1Q2J show appreciable temperature-dependence. The C-C scission reactions of hydroperoxyalkyl radicals are the slowest at temperatures lower than 1100 K. Note that some rate coefficients cease to exist above ~800 K at this pressure, because at least one of the participating species is reacting faster than the slowest timescale corresponding to internal energy relaxation via collisions. In this regime it is not possible to establish a phenomenological (i.e., time-independent) rate coefficient [59, 66-68], instead, the rapidly equilibrating species are merged automatically by MESS, preserving the validity of the rest of the rate coefficients. In the CHEMKIN simulations rate coefficients are represented via Arrhenius fits, which do not have a temperature cut-off. However, because both the formation and the decomposition of these species are very rapid at higher temperatures, their concentrations are also very low, therefore, the exact value of the rate coefficients is of little importance.



**Figure 5.** Temperature-dependence of the calculated rate constants on the cyclopentyl + O<sub>2</sub> PES at a pressure of 10 bar. Panels (a), (b), (c) and (d) show reactions of CYC5H9+O<sub>2</sub>, CPT02J, CPT1Q2J and CPT1Q3J species, respectively. Some rate coefficients do not exist at 10 bar above ~800 K due to well-merging, see text.

The pressure-dependence of the rate constants is shown in Figure 6 at 750 K, a temperature where transition from low- to high-temperature chemistry occurs. Curves corresponding to reactions of CYC5H9+O<sub>2</sub>, CPTO2J, CPT1Q2J and CPT1Q3J species are depicted in Figures 6a, 6b, 6c and 6d, respectively. Figure 6a shows that stabilization of the cyclopentyl + O<sub>2</sub> adduct to the cyclopentyl peroxy radical is the most important channel, even at pressures as low as 0.01 bar, and it becomes more so with increasing pressure. At 0.001 bar, the formally direct pathway of CYC5H9+O<sub>2</sub> going to CYC5H8+HO<sub>2</sub> is faster than the stabilization of the cyclopentyl + O<sub>2</sub> adduct. The formally direct reactions shown in Figure 6a exhibit appreciable pressure dependence between 1 and 100 bar, conditions relevant to turbines and internal combustion engines, with a trend of increase in rate constants at lower pressures. Meanwhile, the rate constants of sequential reactions increase with increasing pressure, particularly between 0.001 and 1 bar. Not surprisingly, the ignition delay times of cyclopentane/air mixtures are highly sensitive to the rates of the investigated reactions, and, therefore, influenced by the pressure-dependence of the rate coefficients as discussed in [42]. This emphasizes the necessity of using accurate pressure-dependent rate coefficients in combustion mechanisms, and including both sequential and formally direct rate coefficients calculated in a rigorous master equation framework. Also note the absence of some rate coefficients at low pressures at 750 K due to species merging. In general, merging is expected to be more prevalent with increasing temperature and decreasing pressures.



**Figure 6.** Pressure-dependence of the calculated rate constants on the cyclopentyl + O<sub>2</sub> PES at a temperature of 750 K. Panels (a), (b), (c) and (d) show reactions of CYC5H9+O<sub>2</sub>, CPTO2J, CPT1Q2J and CPT1Q3J species, respectively.

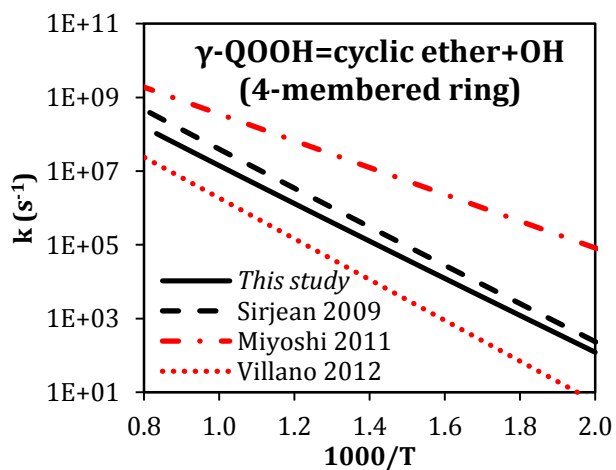
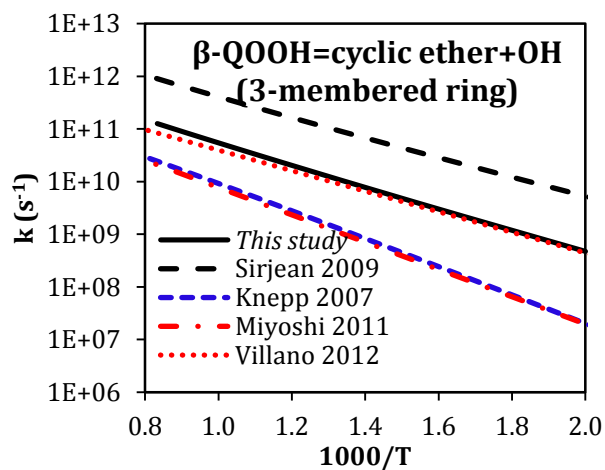
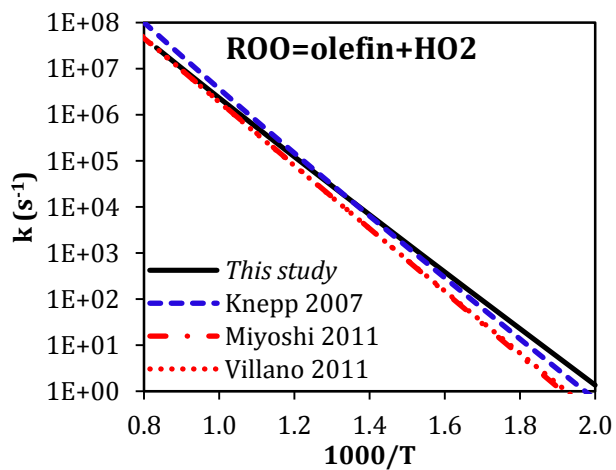
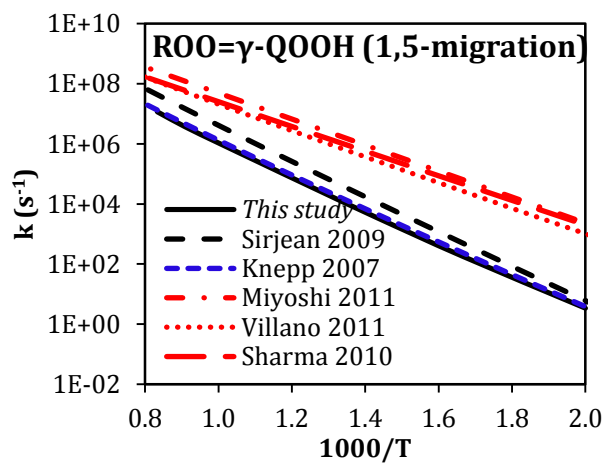
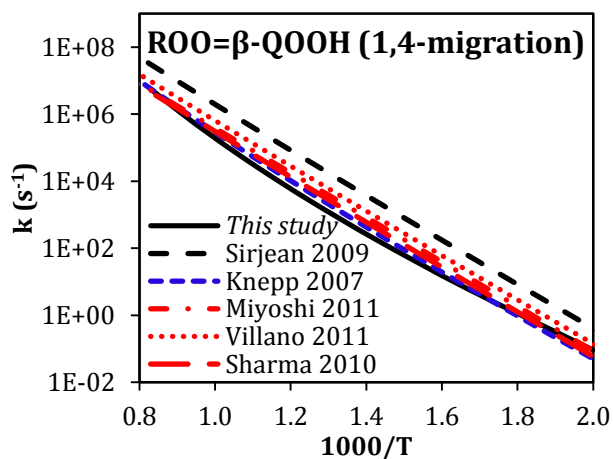
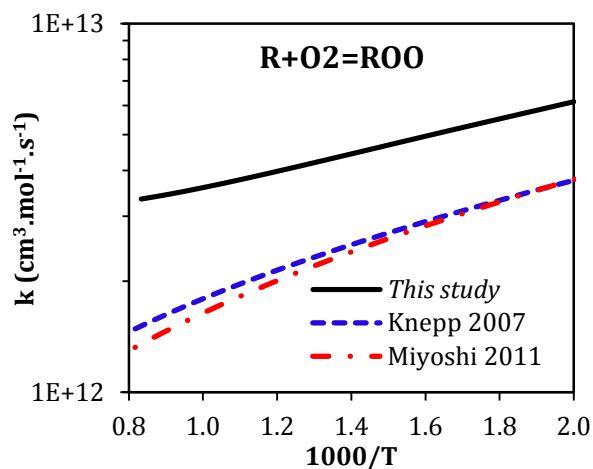
Note that some rate coefficients do not exist below ~1 bar at 750 K. For details see text.

### 5.3. Comparison of rate constants

To the best of our knowledge, only Sirjean et al. [25] investigated the low-temperature kinetics of cyclopentane oxidation. However, the reactions that were covered in their study are limited to the alkylperoxy $\leftrightarrow$ hydroperoxyalkyl isomerization and the formation of cyclic ethers, at their high pressure limit. The rate constants calculated in this study at the UCCSD(T) level of theory are compared to theirs [25] reported at the CBS-QB3 level in Figure 7. Our results are also compared to the high-pressure limit rate constants of analogous reactions falling on the PES of cyclohexyl + O<sub>2</sub> [12], which were also determined using detailed *ab initio* calculations combined with master equation calculations, and were additionally validated against measurements of OH and HO<sub>2</sub> formation at the sub-mechanism level [12]. Furthermore, comparisons are made against the rate constants of analogous reactions for acyclic alkanes from Miyoshi [65], Sharma et al. [51] and Villano et al. [69, 70]. Miyoshi uses the CBS-QB3 quantum mechanical method to evaluate the rate constants for concerted HO<sub>2</sub> elimination and isomerization of the peroxy radicals, as well as the cyclic ether formation and  $\beta$ -scission of the hydroperoxyalkyl radicals [65]. Similarly, Sharma et al. report rules for the H-migration reactions of ROO radicals and the isomerization of OOQOOH species leading to ketohydroperoxides [51] at the CBS-QB3, G2 and MP2/CBSB7 levels. Finally, Villano et al. present high-pressure estimation rules for the reactions investigated by [65] and [51], using CBS-QB3 calculations [69, 70]. In these works the rate coefficients are parameterized based on the chemical nature of the reaction site (primary, secondary or tertiary) and the ring size of transition states (isomerization reactions) or products (cyclic ether formation) are taken into account.

As seen in Figure 7, the calculated rate constants of O<sub>2</sub>-addition to cyclopentyl radical are faster than those for cyclohexyl radical [12] and secondary non-cyclic radicals [65], by up to a factor of 5. The rate constants of H-migration, although similar to those of analogous migration reactions of cyclohexane, are appreciably different from those calculated for the same reactions at the CBS-QB3 level of theory in [25], particularly the 1,4-migration to CPT1Q2J. Figure 8 depicts the variation of the 1,5/1,4 H-migration branching ratio as a function of inverse temperature using rate constants from this study as well as from [25] and [12]. All three sets of values favor the 1,5-migration over the 1,4-migration between 500 K and 1200 K. However, our values, as well as those reported by [12] for the cyclohexane counterparts, yield branching ratios that are up to 4 times greater than those obtained from [25] for cyclopentane. Moreover, the

1,5/1,4 H-migration branching ratios of cyclopentylperoxy calculated using rate constants from [25] exhibit less variations as a function of temperature than those calculated using analogous rate constants of cyclohexylperoxy [12], as well as those determined in this study. For non-cyclic alkanes, the 1,5 migration is much faster than for the cyclic counterpart, and much more favored than the 1,4 migration. The inhibition of the 6-membered ring 1,5 migration in cycloalkanes may be attributed to the energy constraints caused by the geometry distortions, which are required to form the transition state as shown in Figure 9. The C1C2C3 angle bends from 104° (tetrahedral geometry) to 99° in order to get the radical center and oxygen atom close together. The inhibition of this reaction that is involved in low-temperature chain branching is one of the main reasons behind the reduced reactivity of cycloalkanes compared to non-cyclic alkanes. As for the concerted HO<sub>2</sub>-elimination of CPTO2J, at temperatures lower than 1000 K (Figure 7), it is slightly faster than the analogous reactions of non-cyclic alkanes. However, the lower rates of ROO/QOOH isomerization reactions in cyclopentane leads to higher rates of production of HO<sub>2</sub> radicals relative to non-cyclic species. As discussed in [28], high concentrations of HO<sub>2</sub> radicals at rich conditions are responsible for the inhibition of cyclopentane reactivity at intermediate temperatures (800 - 950 K). The calculated formation rate constants of CPTYO13 cyclic ether are relatively similar to those reported by Sirjean et al. [25] (up to 3 times slower). However, Sirjean et al.'s [25] rate constants of the 3-membered ring cyclic ether formation (CPTYO12) are approximately one order of magnitude greater than those determined in our study, due to differences in pre-exponential factors, despite that activation energies are only less than 1 kcal mol<sup>-1</sup> different. Figure 7 shows that there exist significant discrepancies in the rate constants of 3- and 4-membered ring cyclic ether formation reactions, even for acyclic fuels. The C-C β-scission rate constants are compared to those of the relevant rate rule from Villano et al. [70]. The rate constants of CPT1Q3J=C<sub>4</sub>H<sub>7</sub>CHO1-4+OH are compared to analogous values from Refs. [12] and [65] as well. The comparison clearly shows that the dissociation of hydroperoxycyclopentyl radicals is slower than that of the non-cyclic counterpart. It is also slower than the dissociation of analogous hydroperoxycyclohexyl radicals. Consequently, these reactions will have little effect on cyclopentane reactivity. Finally, the HO<sub>2</sub>-elimination from CPT1Q2J leading to cyclopentene has rate constants that are almost one order of magnitude higher than those reported by Miyoshi [65] and Villano et al. [69, 70] for non-cyclic alkanes or by Knepp et al. [12] for cyclohexane, between 500 K and 1200 K.



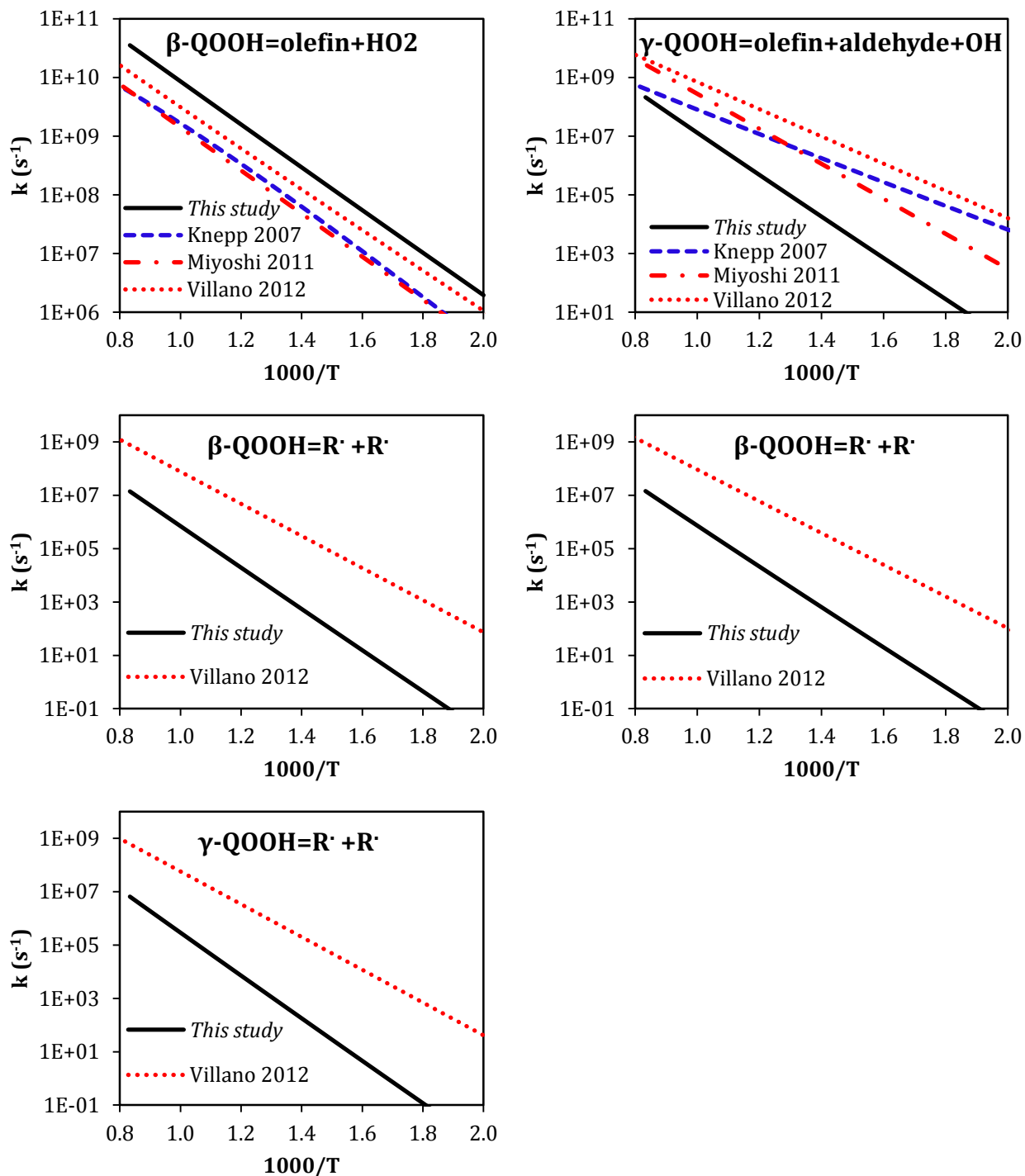


**Figure 7.** Comparison of the high-pressure limit rate constants calculated in this study to those available in the literature for cyclopentane (Sirjean [25]) (black), cyclohexane (Knepp [12]) (blue), and non-cyclic alkanes ([12, 51, 65, 69, 70]) (red) (the cyclopentane-relevant degeneracy of each reaction is taken into account). Note that the differences are largely due to the differences in the chemical systems themselves for which these characteristic rate coefficients were calculated.

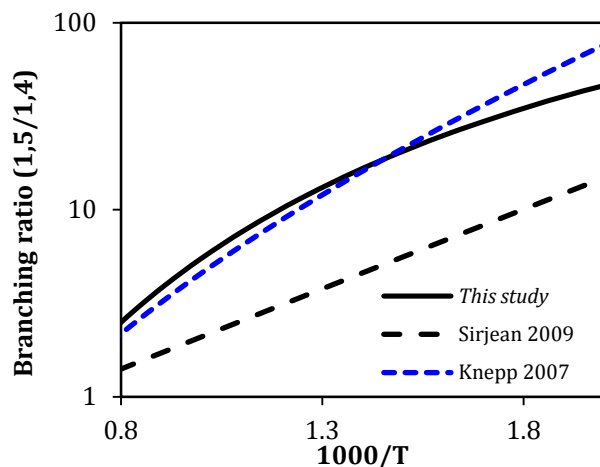


**Figure 8.** Comparison of the 1,5/1,4 H-migration branching ratio profiles of the CPTO2J radical using rate constants determined in [25] (Sirjean 2009), [12] (Knepp 2007), and this study. Black and blue colors are used to distinguish between cyclopentane and cyclohexane data, respectively.

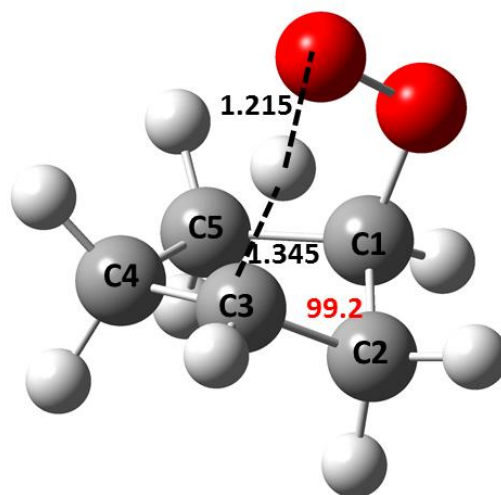


**Figure 9.** Optimized geometry of the 6-membered ring alkylperoxy/hydroperoxyalkyl isomerization. Values in black represent distances in Angstrom and the value in red represents the C1C2C3 angle

#### 5.4. Comparison with Cyclopentyl+O<sub>2</sub> photolysis measurements

De Sain and Taatjes [71] measured HO<sub>2</sub> radical profiles generated during the reaction of cyclopentyl radical with O<sub>2</sub> using laser flash photolysis at temperatures between 296-723 K. The

authors found two distinct components to the HO<sub>2</sub> production, the first is a near-instantaneous prompt production and the second is a slower rise in HO<sub>2</sub> signal. We utilized the present kinetic model to simulate the experimental work by De Sain and Taatjes [71]. The total gas density was fixed to those in the experiments, and we assumed that all cyclopentane was converted to cyclopentyl radical by reaction with Cl in the experiments. In this way, our simulations predict HO<sub>2</sub> mole fractions as a function of time at various initial temperature conditions.

Our simulation results showed excellent qualitative agreement with the experiments of De Sain and Taatjes. At temperatures below 453 K, the simulations did not show significant HO<sub>2</sub> production, which was also observed in the experiments. As the temperature increased above 500 K, there was discernible increase in HO<sub>2</sub> production. Two distinct regions of HO<sub>2</sub> production were observed, first a rapid prompt formation that occurred in several tens to hundreds of microseconds, which was followed by a slower rise that continued for several milliseconds. The total HO<sub>2</sub> mole fraction at various temperatures, as well as the prompt HO<sub>2</sub> mole fraction profiles are shown in Figure 10. Similar to the experiments, the simulations show an increase in total HO<sub>2</sub> mole fraction with increasing temperature. The HO<sub>2</sub> produced via the prompt mechanism is considerably smaller than the total, and we observe a general increase with increasing temperature. Note, it was difficult to differentiate between the prompt and slow formation of HO<sub>2</sub> in the higher temperature simulations because the change in slope is not always clear. A rate of production analysis performed at early times, corresponding to the prompt formation region, indicated that HO<sub>2</sub> was entirely formed via the concerted reaction of cyclopentyl+O<sub>2</sub>=cyclopentene+HO<sub>2</sub>. At later times, corresponding to the slow formation region, HO<sub>2</sub> is still produced by concerted elimination, but also by cyclopentylperoxy (RO<sub>2</sub>) radical decomposition to smaller species leading to HCO+O<sub>2</sub>=HO<sub>2</sub>+CO.

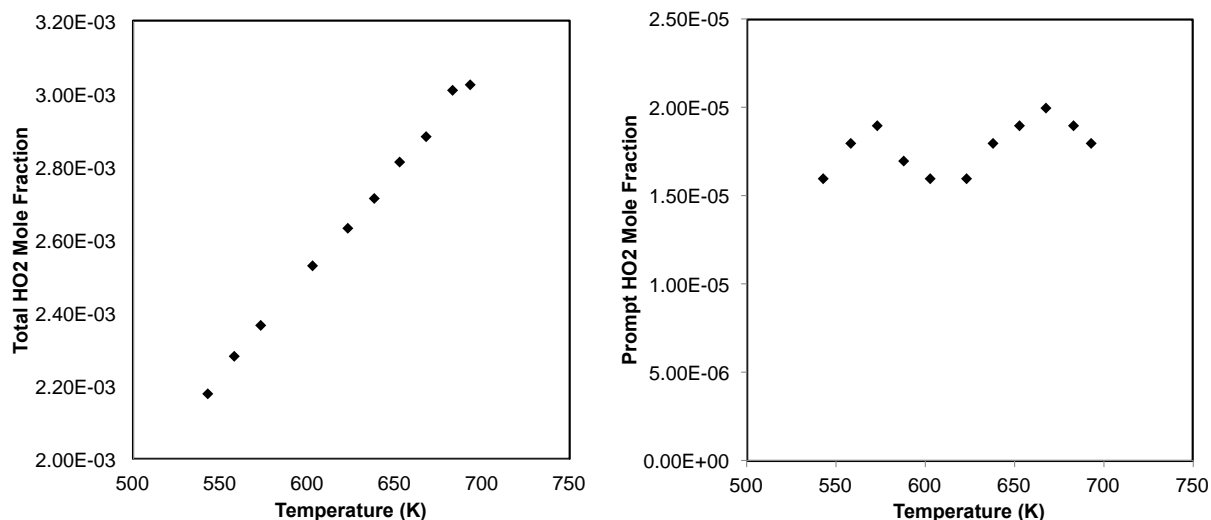


**Figure 10.** Total (left) and prompt (right) HO<sub>2</sub> radical mole fractions as a function of temperature for cyclopentyl+O<sub>2</sub> at a constant total density of  $8.5 \times 10^{17}$  molecule cm<sup>-3</sup>.

### 5.5. Pressure Effects

To evaluate the importance of pressure-dependence at low pressures and its influence on reactivity, simulations of a constant volume homogeneous batch reactor were run at  $\phi=1$ ,  $600 < T < 1200$  K and pressures of 1, 5, 10, 50 and 100 bar using two versions of the model: i) the original one “P-dep” and ii) one with rate coefficients of sequential low-temperature oxidation pathways only at the high-pressure limit “HP”, and no formally direct pathways. The simulated ignition delay time (IDT) corresponds to the time at which  $dT/dt$  is maximum. As shown in Figure 11, pressure-dependence effects are not very important at pressures greater than 50 bar where rate constants approach the high-pressure limit. Meanwhile, the data at 5 and 10 bar show that pressure dependence increases reactivity for temperatures greater than 1000 K, and slightly decreases reactivity between 600 and 800 K. The decrease in reactivity at low temperatures is expected, and is due to lower rates of sequential reactions when pressure-dependent rate parameters are used. Based on a brute force sensitivity analysis run at 20 bar, 1100 K and  $\phi=1$  (refer to part II [42]), the increase in reactivity at  $T > 1000$  K is mainly due to the CYC5H9+O<sub>2</sub>=CYC5H8+HO<sub>2</sub> reaction. The fact that a reaction producing un-reactive species increases reactivity is due to the fact that the HO<sub>2</sub> radicals produced at high temperatures are converted to H<sub>2</sub>O<sub>2</sub> which dissociates into two OH radicals. Surprisingly, this effect is not observed at P=1 bar. Temperature sensitivity analyses,  $dT/dk_i$ , were conducted at  $\phi=1$ , T=1100 K and pressures of 1 and 5 bar using both versions of the model in order to determine why

pressure-dependence is not observed at P=1 bar. The results calculated just before ignition are shown in Figure 12 where positive sensitivity coefficients indicate an increase in temperature and reactivity with increasing reaction rates, and vice versa. At 1 bar, the reactivity of “P-dep” and “HP” models is sensitive to the same set of reactions, with reactions involving resonantly stabilized species such as allyl, cyclopentadienyl and 1,3-pentadien-5-yl (C\*CC\*CCJ) radicals being among the most sensitive reactions. Meanwhile, at 5 bar, greater differences are observed in the sensitivity trends of the two models with the low-temperature oxidation reaction CPTO2J=CYC5H8+HO2 being much more sensitive at “HP” conditions. Other reactions involving HO<sub>2</sub> radicals, such as CPT+HO<sub>2</sub>=CYC5H9+H<sub>2</sub>O<sub>2</sub>, 2HO<sub>2</sub>=H<sub>2</sub>O<sub>2</sub>+O<sub>2</sub> and C<sub>3</sub>H<sub>5</sub>-A+HO<sub>2</sub>=C<sub>3</sub>H<sub>5</sub>O+OH, are more sensitive at “P-dep” conditions where the concentration of HO<sub>2</sub> radicals is different than that at “HP” due to the formally direct pathway CYC5H<sub>9</sub>+O<sub>2</sub>=CYC5H<sub>8</sub>+HO<sub>2</sub>, which is included only in the “P-dep” model. It should be noted that this pathway is highly sensitive at 5 bar, but less so at 1 bar. The different behavior at the seemingly similar conditions is likely caused by an overall change in the oxidation regime. When the H<sub>2</sub>O<sub>2</sub>(+ M) = 2 OH (+ M) reaction becomes fast enough to generate a significant amount of OH, HO<sub>2</sub>-related reactions will also gain importance, since HO<sub>2</sub> is the primary source of H<sub>2</sub>O<sub>2</sub>. At 5 bar, roughly, both the H<sub>2</sub>O<sub>2</sub> and the M number densities are 5 times larger, which makes the rate of the reaction 25 times faster, and 25 times more important of an OH source. Overall, the results obtained herein emphasize the importance of using pressure-dependent rate coefficients for accurate prediction of reactivity trends, and exemplifies the need why mechanisms should be tested in a wide pressure and temperature range.

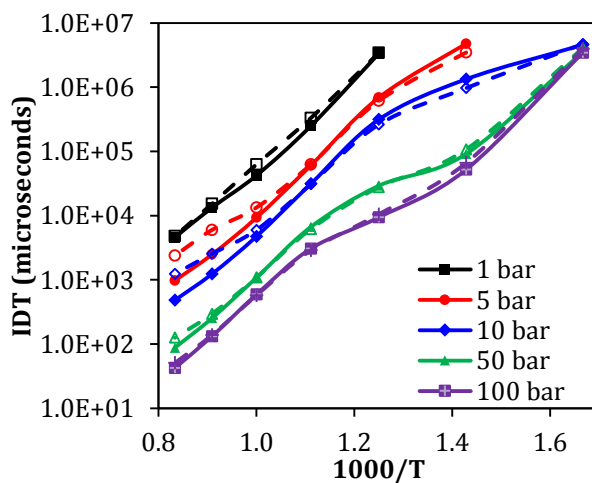


**Figure 11.** Effect of pressure-dependence of low-temperature oxidation pathways on cyclopentane reactivity (solid and dashed lines correspond to simulations with and without pressure-dependence, respectively)

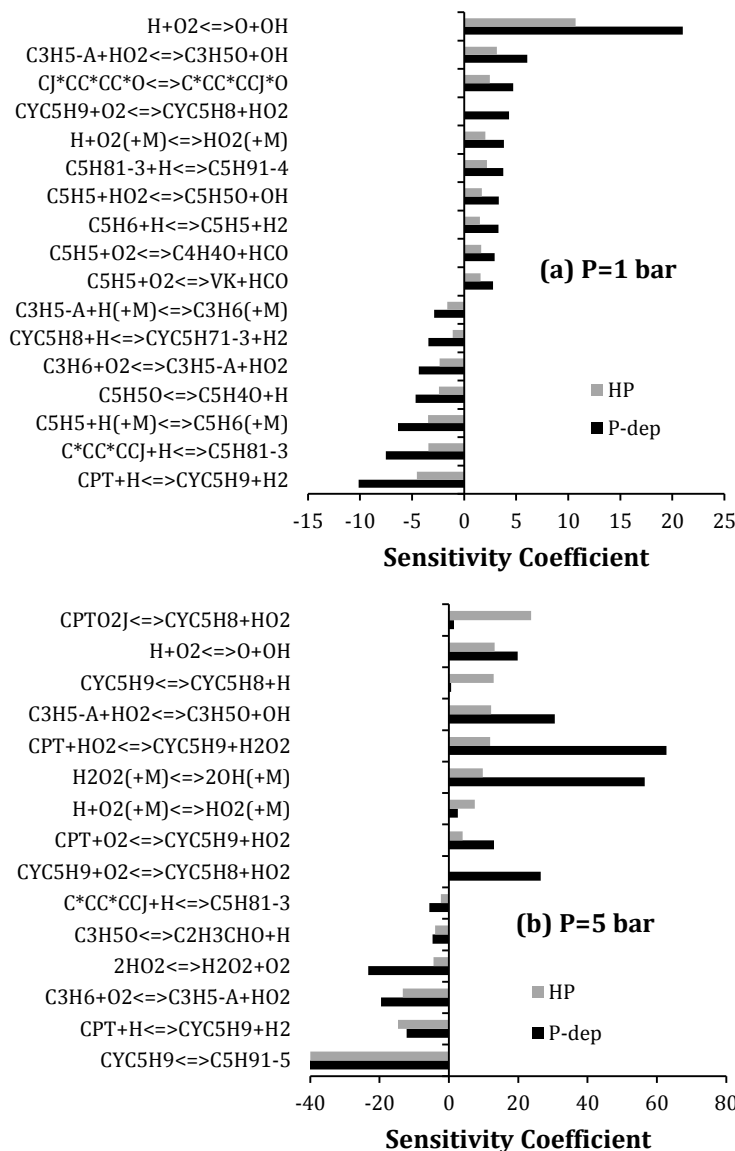


**Figure 12.** Temperature-sensitivity analyses at  $\phi=1$ ,  $T=1100\text{K}$  and pressures of 1 (a) and 5 bar (b) using the two versions of the model.

## 6. Conclusion

A detailed kinetic mechanism of high- and low-temperature cyclopentane oxidation was developed for the first time using rate coefficients available in the literature as well as analogies.

Due to the lack of reliable kinetic data pertaining to low-temperature reactivity, the temperature- and pressure-dependent rate coefficients of elementary reactions lying on the potential energy surface of cyclopentyl + O<sub>2</sub> were determined using high level electronic structure calculations and RRKM-based master equation analysis. The results show that the rate coefficients are strongly pressure-dependent, that the importance of formally direct rate coefficients are comparable to sequential ones even at 10 bar, and that many of the investigated reactions are in the falloff even at 1 bar. In particular, the formally direct pathway  $\text{CYC5H9} + \text{O}_2 = \text{CYC5H8} + \text{HO}_2$  is very important in the pressure range of 5 to 10 bar and for temperatures above 1000K. Comparisons of the calculated rate constants with analogous rate coefficients for non-cyclic alkanes suggest that these are the reactions that are responsible for the reduced reactivity of cycloalkanes. Our results show that this is mainly due to the suppression of the peroxy 1,5 H-migration pathway. The barrier heights on the cyclopentyl + O<sub>2</sub> PES calculated in this study are similar to those calculated by Sirjean et al. [25] for the same reactions at a lower level of theory. However, the rate constants are different in the two studies mainly due to the treatments of kinetic details and the overall master equation model. The computed rate coefficients are used in the detailed mechanism that is validated against new cyclopentane ignition data as well as data available in the literature. These experimental and modeling results are detailed in the second part of this study.

### **Acknowledgements**

The authors would like to acknowledge Dr. Judit Zador for her valuable support and feedback. This work was performed by the Clean Combustion Research Center with funding from King Abdullah University of Science and Technology (KAUST) and Saudi Aramco under the FUELCOM program. Research reported in this publication was also supported by competitive research funding from KAUST. The work at LLNL was supported by the U.S. Department of Energy, Vehicle Technologies Office, program managers Gurpreet Singh and Leo Breton and was performed under the auspices of the U.S. Department of Energy by Lawrence Livermore National Laboratories under contract DE-AC52-07NA27344.

## References

- [1] C.J. Mueller, W.J. Cannella, T.J. Bruno, B. Bunting, H.D. Dettman, J.A. Franz, M.L. Huber, M. Nataraja, W.J. Pitz, M.A. Ratcliff, K. Wright, Methodology for Formulating Diesel Surrogate Fuels with Accurate Compositional, Ignition-Quality, and Volatility Characteristics, *Energy Fuels* 26 (2012) 3284–3303.
- [2] W.J. Pitz, C.J. Mueller, Recent progress in the development of diesel surrogate fuels, *Progress in Energy and Combustion Science* 37 (2011) 330-350.
- [3] S. Dooley, S.H. Won, M. Chaos, J. Heyne, Y. Ju, F.L. Dryer, K. Kumar, C.-J. Sung, H. Wang, M.A. Oehlschlaeger, R.J. Santoro, T.A. Litzinger, A jet fuel surrogate formulated by real fuel properties, *Combust. Flame* 157 (2010) 2333-2339.
- [4] S. Dooley, S.H. Won, J. Heyne, T.I. Farouk, Y. Ju, F.L. Dryer, K. Kumar, C.-J. Sung, H. Wang, M.A. Oehlschlaeger, V. Iyer, T.A. Litzinger, R.J. Santoro, T. Malewicki, K. Brezinsky, The experimental evaluation of a methodology for surrogate fuel formulation to emulate gas phase combustion kinetic phenomena, *Combust. Flame* 159 (2012) 1444-1466.
- [5] S.M. Sarathy, G. Kukkadapu, M. Mehl, T. Javed, A. Ahmed, N. Naser, A. Tekawade, G. Kosiba, M. Abbad, E. Singh, S. Park, M. Al Rashidi, W.L. Roberts, M.A. Oehlschlaeger, C.-J. Sung, A. Farooq, Compositional effects on the ignition of FACE gasoline fuels, *Combust. Flame*, (2016).
- [6] C.S. McEnally, L.D. Pfefferle, Experimental study of fuel decomposition and hydrocarbon growth processes for cyclohexane and related compounds in nonpremixed flames, *Combust. Flame* 136 (2004) 155-167.
- [7] Y. Yang, A.L. Boehman, J.M. Simmie, Effects of molecular structure on oxidation reactivity of cyclic hydrocarbons: Experimental observations and conformational analysis, *Combust. Flame* 157 (2010) 2369-2379.
- [8] Y. Yang, A.L. Boehman, J.M. Simmie, Uniqueness in the low temperature oxidation of cycloalkanes, *Combust. Flame* 157 (2010) 2357-2368.
- [9] B.W. Weber, W.J. Pitz, M. Mehl, E.J. Silke, A.C. Davis, C.-J. Sung, Experiments and modeling of the autoignition of methylcyclohexane at high pressure, *Combust. Flame* 161 (2014) 1972-1983.
- [10] C.K. Westbrook, Challenges in Combustion. Meeting the Challenge of Reducing Global GHG Emissions through Energy Research. [http://gcep.stanford.edu/pdfs/uQx8GXJG882-3q6NMuyQOw/westbrook\\_symp05.pdf](http://gcep.stanford.edu/pdfs/uQx8GXJG882-3q6NMuyQOw/westbrook_symp05.pdf).
- [11] R.X. Fernandes, J. Zador, L.E. Jusinski, J.A. Miller, C.A. Taatjes, Formally direct pathways and low-temperature chain branching in hydrocarbon autoignition: the cyclohexyl + O<sub>2</sub> reaction at high pressure, *Phys. Chem. Chem. Phys.* 11 (2009) 1320-1327. <http://www.ncbi.nlm.nih.gov/pubmed/19224032>
- [12] A.M. Knepp, G. Meloni, L.E. Jusinski, C.A. Taatjes, C. Cavallotti, S.J. Klippenstein, Theory, measurements, and modeling of OH and HO<sub>2</sub> formation in the reaction of cyclohexyl radicals with O<sub>2</sub>, *Phys. Chem. Chem. Phys.* 9 (2007) 4315-4331.
- [13] W.J. Pitz, C.V. Naik, T.N. Mhaoldúin, C.K. Westbrook, H.J. Curran, J.P. Orme, J.M. Simmie, Modeling and experimental investigation of methylcyclohexane ignition in a rapid compression machine, *Proc. Combust. Inst.* 31 (2007) 267-275.
- [14] E.J. Silke, W.J. Pitz, C.K. Westbrook, M. Ribaucour, Detailed chemical kinetic modeling of cyclohexane oxidation, *J. Phys. Chem. A* 111 (2007) 3761-3775.

- [15] B. Sirjean, F. Buda, H. Hakka, P.A. Glaude, R. Fournet, V. Warth, F. Battin-Leclerc, M. Ruiz-Lopez, The autoignition of cyclopentane and cyclohexane in a shock tube, *Proc. Combust. Inst.* 31 (2007) 277-284.
- [16] Z. Tian, C. Tang, Y. Zhang, J. Zhang, Z. Huang, Shock Tube and Kinetic Modeling Study of Cyclopentane and Methylcyclopentane, *Energy Fuels* 29 (2015) 428-441.
- [17] W. Tsang, Thermal decomposition of cyclopentane and related compound, *Int. J. Chem. Kin.* 10 (1978) 599-617.
- [18] A.T. Droege, F.P. Tully, Hydrogen atom abstraction from alkanes by OH. 6. Cyclopentane and cyclohexane, *J. Phys. Chem.* 91 (1987) 1222-1225.
- [19] S.M. Handford-Styring, R.W. Walker, Addition of cyclopentane to slowly reacting mixtures of H<sub>2</sub>+O<sub>2</sub> between 673 and 783 K: Reactions of H and OH with cyclopentane and cyclopentyl radicals, *J. Chem. Soc., Faraday Trans.* 91 (1995) 1431-1438.
- [20] R. Sivaramakrishnan, J.V. Michael, Shock tube measurements of high temperature rate constants for OH with cycloalkanes and methylcycloalkanes, *Combust. Flame* 156 (2009) 1126-1134.
- [21] I.A. Awan, D.R. Burgess Jr, W. Tsang, J.A. Manion, Shock tube study of the decomposition of cyclopentyl radicals, *Proc. Combust. Inst.* 33 (2011) 341-349.
- [22] B. Sirjean, P.A. Glaude, M. Ruiz-Lopez, R. Fournet, Detailed kinetic study of the ring opening of cycloalkanes by CBS-QB3 calculations, *J. Phys. Chem. A* 110 (2006) 12693-12704.
- [23] W. Tsang, Mechanism and Rate Constants for the Decomposition of 1-Pentenyl Radicals, *J. Phys. Chem. A* 110 (2006) 8501-8509.
- [24] K. Wang, S.M. Villano, A.M. Dean, Reactions of allylic radicals that impact molecular weight growth kinetics, *Phys. Chem. Chem. Phys.* 17 (2015) 6255.
- [25] B. Sirjean, P.A. Glaude, M. Ruiz-Lopez, R. Fournet, Theoretical kinetic study of the reactions of cycloalkylperoxy radicals, *J. Phys. Chem. A* 113 (2009) 6924-6935.
- [26] S.M. Sarathy, C.K. Westbrook, M. Mehl, W.J. Pitz, C. Togbe, P. Dagaut, H. Wang, M.A. Oehlschlaeger, U. Niemann, K. Seshadri, P.S. Veloo, C. Ji, F.N. Egolfopoulos, T. Lu, Comprehensive chemical kinetic modeling of the oxidation of 2-methylalkanes from C7 to C20, *Combust. Flame* 158 (2011) 2338-2357.
- [27] S.M. Burke, W. Metcalfe, O. Herbinet, F. Battin-Leclerc, F.M. Haas, J. Santner, F.L. Dryer, H.J. Curran, An experimental and modeling study of propene oxidation. Part 1: Speciation measurements in jet-stirred and flow reactors, *Combust. Flame* 161 (2014) 2765-2784.
- [28] M.J. Al Rashidi, S. Thion, C. Togbé, G. Dayma, M. Mehl, P. Dagaut, W.J. Pitz, J. Zádor, S.M. Sarathy, Elucidating reactivity regimes in cyclopentane oxidation: jet stirred reactor experiments, computational chemistry, and kinetic modeling (submitted), *Proc. Combust. Inst.*, (May 2016).
- [29] F. Agapito, P.M. Nunes, B.J. Costa Cabral, R.M. Borges dos Santos, J.A. Martinho Simoes, Energetic differences between the five- and six-membered ring hydrocarbons: strain energies in the parent and radical molecules, *J. Org. Chem.* 73 (2008) 6213-6223.
- [30] E.R. Ritter, J.W. Bozzelli, THERM: Thermodynamic property estimation for gas phase radicals and molecules, *Int. J. Chem. Kin.* 23 (1991) 767-778.
- [31] O.V. Dorofeeva, L.V. Gurvich, V.S. Jorish, Thermodynamic Properties of Twenty-One Monocyclic Hydrocarbons, *J. Phys. Chem. Ref. Data* 15 (1986) 437-464.

- [32] D.L. Allara, R. Shaw, A compilation of kinetic parameters for the thermal degradation of n-alkane molecules, *J. Phys. Chem. Ref. Data* 9 (1980) 523-559.
- [33] D.K. Lewis, J. Bergmann, R. Manjoney, R. Paddock, B.L. Kaira, Rates of reactions of cyclopropane, cyclobutane, cyclopentene, and cyclohexene in the presence of boron trichloride, *J. Phys. Chem.* 88 (1984) 4112-4116.
- [34] R. Atkinson, Kinetics of the gas-phase reactions of OH radicals with alkanes and cycloalkanes, *Atmos. Chem. Phys.* 3 (2003) 2233-2307.
- [35] J.F. Bott, N. Cohen, A shocktube study of the reaction of the hydroxyl radical with H<sub>2</sub>, CH<sub>4</sub>, *c*-C<sub>5</sub>H<sub>10</sub> and *i*-C<sub>4</sub>H<sub>10</sub>, *Int. J. Chem. Kin.* 21 (1989) 485-498.
- [36] W.B. DeMore, K.D. Bayes, Rate constants for the reactions of hydroxyl radical with several alkanes, cycloalkanes and dimethylether, *J. Phys. Chem. A* 103 (1999) 2649-2654.
- [37] M.A. Gennaco, Y.W. Huang, R.A. Hannun, T.J. Dransfield, Absolute rate constants for the reaction of OH with cyclopentane and cycloheptane from 233 to 351 K, *J Phys Chem A* 116 (2012) 12438-12443. <http://www.ncbi.nlm.nih.gov/pubmed/23194446>
- [38] F. Kramp, S.E. Paulson, On the uncertainties in the rate coefficients for OH reactions with hydrocarbons, and rate coefficients of 1,3,5-trimethylbenzene and *m*-xylene reactions with OH radicals in the gas phase, *J. Phys. Chem. A* 102 (1998) 2685-2690.
- [39] S. Singh, M.F. de Leon, Z. Li, Kinetics study of the reaction of OH radicals with C5-C8 cycloalkanes at 240-340 K using the relative rate/discharge flow/mass spectrometry technique, *J Phys Chem A* 117 (2013) 10863-10872. <http://www.ncbi.nlm.nih.gov/pubmed/24053620>
- [40] E.W. Wilson, W.A. Hamilton, H.R. Kennington, B. Evans, N.W. Scott, W.B. DeMore, Measurements and estimation of rate constants for the reactions of hydroxyl radical with several alkanes and cycloalkanes, *J. Phys. Chem. A* 110 (2006) 3593-3604.
- [41] M. Mehl, G. Vanhove, W.J. Pitz, E. Ranzi, Oxidation and combustion of the n-hexene isomers: A wide range kinetic modeling study, *Combust. Flame* 155 (2008) 756-772.
- [42] M. Al Rashidi, J. Calero, C. Banyon, M.B. Sajid, M. Mehl, W.J. Pitz, J. Zador, H.J. Curran, A. Farooq, S.M. Sarathy, Cyclopentane combustion. Part II. Ignition delay measurements and mechanism validation (submitted), *Combust. Flame*, (May 2016).
- [43] D.M. Matheu, W.H. Green, J.M. Grenda, Capturing pressure-dependence in automated mechanism generation: Reactions through cycloalkyl intermediates, *Int. J. Chem. Kin.* 35 (2003) 95-119.
- [44] S. Sharma, S. Raman, W.H. Green, Intramolecular Hydrogen Migration in Alkylperoxy and Hydroperoxyalkylperoxy Radicals: Accurate Treatment of Hindered Rotors, *J. Phys. Chem. A* 114 (2010) 5689-5701.
- [45] H.J. Curran, Rate constant estimation for C1 to C4 alkyl and alkoxy radical decomposition, *Int. J. Chem. Kin.* 38 (2006) 250-275.
- [46] Y. Yang, A.L. Boehman, Experimental study of cyclohexane and methylcyclohexane oxidation at low to intermediate temperature in a motored engine, *Proc. Combust. Inst.* 32 (2009) 419-426.
- [47] Y. Yang, A.L. Boehman, Oxidation chemistry of cyclic hydrocarbons in a motored engine: Methylcyclopentane, tetralin, and decalin, *Combust. Flame* 157 (2010) 495-505.
- [48] Z. Serinyel, O. Herbinet, O. Frottier, P. Dirrenberger, V. Warth, P.A. Glaude, F. Battin-Leclerc, An experimental and modeling study of the low- and high-temperature oxidation of cyclohexane, *Combust. Flame* 160 (2013) 2319-2332.

- [49] S. Vranckx, C. Lee, H.K. Chakravarty, R.X. Fernandes, A rapid compression machine study of the low temperature combustion of cyclohexane at elevated pressures, *Proc. Combust. Inst.* 34 (2013) 377-384.
- [50] C.F. Goldsmith, W.H. Green, S.J. Klippenstein, Role of O<sub>2</sub> + QOOH in low-temperature ignition of propane. 1. Temperature and pressure dependent rate coefficients, *J. Phys. Chem. A* 116 (2012) 3325-3346.
- [51] S. Sharma, S. Raman, W.H. Green, Intramolecular hydrogen migration in alkylperoxy and hydroperoxyalkylperoxy radicals: accurate treatment of hindered rotors, *J. Phys. Chem. A* 114 (2010) 5689-5701.
- [52] A. Jalan, I.M. Alecu, R. Meana-Paneda, J. Aguilera-Iparraguirre, K.R. Yang, S.S. Merchant, D.G. Truhlar, W.H. Green, New pathways for formation of acids and carbonyl products in low-temperature oxidation: the Korcek decomposition of gamma-ketohydroperoxides, *J Am Chem Soc* 135 (2013) 11100-11114.  
<http://www.ncbi.nlm.nih.gov/pubmed/23862563>
- [53] J. Bugler, K.P. Somers, E.J. Silke, H.J. Curran, Revisiting the Kinetics and Thermodynamics of the Low-Temperature Oxidation Pathways of Alkanes: A Case Study of the Three Pentane Isomers, *J Phys Chem A* 119 (2015) 7510-7527.  
<http://www.ncbi.nlm.nih.gov/pubmed/25798548>
- [54] K. Zhang, C. Banyon, C. Togbé, P. Dagaut, J. Bugler, H.J. Curran, An experimental and kinetic modeling study of n-hexane oxidation, *Combust. Flame* 162 (2015) 4194-4207.
- [55] H.-J. Werner, P.J. Knowles, G. Knizia, F.R. Manby, M. Schütz, *WIREs Computational Molecular Science* 2 (2012) 242-253.
- [56] M.J. Frisch, G.W. Trucks, H.B. Schlegel, G.E. Scuseria, M.A. Robb, J.R. Cheeseman, G. Scalmani, V. Barone, B. Mennucci, G.A. Petersson, H. Nakatsuji, M. Caricato, X. Li, H.P. Hratchian, A.F. Izmaylov, J. Bloino, G. Zheng, J.L. Sonnenberg, M. Hada, M. Ehara, K. Toyota, R. Fukuda, J. Hasegawa, M. Ishida, T. Nakajima, Y. Honda, O. Kitao, H. Nakai, T. Vreven, J.A. Montgomery, Jr., J.E. Peralta, F. Ogliaro, M. Bearpark, J.J. Heyd, E. Brothers, K.N. Kudin, V.N. Staroverov, R. Kobayashi, J. Normand, K. Raghavachari, A. Rendell, J.C. Burant, S.S. Iyengar, J. Tomasi, M. Cossi, N. Rega, N.J. Millam, M. Klene, J.E. Knox, J.B. Cross, V. Bakken, C. Adamo, J. Jaramillo, R. Gomperts, R.E. Stratmann, O. Yazyev, A.J. Austin, R. Cammi, C. Pomelli, J.W. Ochterski, R.L. Martin, K. Morokuma, V.G. Zakrzewski, G.A. Voth, P. Salvador, J.J. Dannenberg, S. Dapprich, A.D. Daniels, Ö. Farkas, J.B. Foresman, J.V. Ortiz, J. Cioslowski, D.J. Fox, *Gaussian 09 Revision D.01*, Wallingford, CT, (2009).
- [57] Y. Georgievskii, S.J. Klippenstein, *J. Phys. Chem. A* 107 (2003) 9776-9781.
- [58] Y. Georgievskii, S.J. Klippenstein, *VaReCoF*, Sandia National Laboratories and Argonne National Laboratory, 2006.
- [59] Y. Georgievskii, J.A. Miller, M.P. Burke, S.J. Klippenstein, Reformulation and solution of the master equation for multiple-well chemical reactions, *J. Phys. Chem. A* 117 (2013) 12146-12154.
- [60] L.S. Tee, S. Gotoh, W.E. Stewart, *Ind. Eng. Chem. Fund.* 5 (1966) 356-363.
- [61] S.W. Benson, *Thermochemical Kinetics*, Wiley, New York, 1976.
- [62] C.F. Goldsmith, A.S. Tomlin, S.J. Klippenstein, Uncertainty propagation in the derivation of phenomenological rate coefficients from theory: A case study of propyl radical oxidation, *Proc. Combust. Inst.* 34 (2013) 177-185.
- [63] S. Mohamed, L. Cai, F. Khaled, C. Banyon, Z. Wang, M. Al Rashidi, H. Pitsch, H. Curran, A. Farooq, S.M. Sarathy, *Modeling Ignition of a Heptane Isomer: Improved*

Thermodynamics, Reaction Pathways, Kinetic, and Rate Rule Optimizations for 2-Methylhexane, *J. Phys. Chem. A* jp-2016-009078.R1 (2016).

[64] I. Auzmendi-Murua, J.W. Bozzelli, Thermochemical properties and bond dissociation energies of C3-C5 cycloalkyl hydroperoxides and peroxy radicals: cycloalkyl radical + (3)O<sub>2</sub> reaction thermochemistry, *J Phys Chem A* 116 (2012) 7550-7563.

<https://www.ncbi.nlm.nih.gov/pubmed/22779400>

[65] A. Miyoshi, Systematic computational study on the unimolecular reactions of alkylperoxy (RO<sub>2</sub>), hydroperoxyalkyl (QOOH), and hydroperoxyalkylperoxy (O<sub>2</sub>QOOH) radicals, *J Phys Chem A* 115 (2011) 3301-3325.

<http://www.ncbi.nlm.nih.gov/pubmed/21446694>

[66] J.A. Miller, S.J. Klippenstein, From the multiple-well master equation to phenomenological rate coefficients: Reactions on a C<sub>3</sub>H<sub>4</sub> potential energy surface, *J. Phys. Chem. A* 107 (2003) 2680-2692.

[67] J.A. Miller, S.J. Klippenstein, Master equation methods in gas phase chemical kinetics, *J. Phys. Chem. A* 110 (2006) 10528-10544.

[68] J.A. Miller, S.J. Klippenstein, S.H. Robertson, M.J. Pilling, R. Shannon, J. Zádor, A.W. Jasper, C.F. Goldsmith, M.P. Burke, Comment on "when rate constants are not enough" by John R. Barker, Michael Frenklach, and David M. Golden, *J. Phys. Chem. A* 120 (2016) 306-312.

[69] S.M. Villano, L.K. Huynh, H.H. Carstensen, A.M. Dean, High-pressure rate rules for alkyl + O<sub>2</sub> reactions. 1. The dissociation, concerted elimination, and isomerization channels of the alkyl peroxy radical, *J Phys Chem A* 115 (2011) 13425-13442.

<http://www.ncbi.nlm.nih.gov/pubmed/22003961>

[70] S.M. Villano, L.K. Huynh, H.H. Carstensen, A.M. Dean, High-pressure rate rules for alkyl + O<sub>2</sub> reactions. 2. The isomerization, cyclic ether formation, and  $\beta$ -scission reactions of hydroperoxy alkyl radicals, *J. Phys. Chem. A* 116 (2012) 5068-5089.

[71] J.D. DeSain, C.A. Taatjes, Infrared Frequency-Modulation Probing of Product Formation in Alkyl + O<sub>2</sub> Reactions: III. The Reaction of Cyclopentyl Radical (c-C<sub>5</sub>H<sub>9</sub>) with O<sub>2</sub> between 296 and 723 K, *J. Phys. Chem. A* 105 (2001) 6646-6654.